

NoSOCS in SDSS. V. Red Disc and Blue Bulge Galaxies Across Different Environments

P. A. A. Lopes^{1*}, S. B. Rembold², A. L. B. Ribeiro³, R. S. Nascimento¹, B. Vajgel⁴

¹ *Observatório do Valongo, Universidade Federal do Rio de Janeiro, Ladeira do Pedro Antônio 43, Rio de Janeiro, RJ, 20080-090, Brazil*

² *Universidade Federal de Santa Maria – 97105-900, Santa Maria-RS, Brazil*

³ *Laboratório de Astrofísica Teórica e Observacional – Departamento de Ciências Exatas e Tecnológicas – Universidade Estadual de Santa Cruz, 45650-000, Ilhéus, BA, Brazil*

⁴ *Observatório Nacional, Rua General José Cristino, 77, Rio de Janeiro, RJ, 20921-400, Brazil*

Accepted 2016 June 20. Received 2016 May 23; in original form 2016 March 12

ABSTRACT

We investigated the typical environment and physical properties of “red discs” and “blue bulges”, comparing those to the “normal” objects in the blue cloud and red sequence. Our sample is composed of cluster members and field galaxies at $z \leq 0.1$, so that we can assess the impact of the local and global environment. We find that disc galaxies display a strong dependence on environment, becoming redder for higher densities. This effect is more pronounced for objects within the virial radius, being also strong related to the stellar mass. We find that local and global environment affect galaxy properties, but the most effective parameter is stellar mass. We find evidence for a scenario where “blue discs” are transformed into “red discs” as they grow in mass and move to the inner parts of clusters. From the metallicity differences of red and blue discs, and the analysis of their star formation histories, we suggest the quenching process is slow. We estimate a quenching time scale of $\sim 2\text{--}3$ Gyr. We also find from the $\text{sSFR}\text{--}M_*$ plane that “red discs” gradually change as they move into clusters. The “blue bulges” have many similar properties than “blue discs”, but some of the former show strong signs of asymmetry. The high asymmetry “blue bulges” display enhanced recent star formation compared to their regular counterparts. That indicates some of these systems may have increased their star formation due to mergers. Nonetheless, there may not be a single evolutionary path for these blue early-type objects.

Key words: surveys – galaxies: clusters: general – galaxies: structure – galaxies: evolution.

1 INTRODUCTION

The environment where galaxies reside have a strong influence on their physical properties (Oemler 1974; Dressler 1980), related to their structure and star formation activity. In a color-magnitude (or color-mass) diagram we can broadly classify local galaxies in two main types. In such diagrams most galaxies are found in two regions, called “blue cloud” (BC) and “red sequence” (RS). The former is mainly composed by late-type galaxies, blue spirals, with high star formation rate (SFR). The latter comprises early-types, elliptical and S0 galaxies, which are redder, bulge-dominated and with negligible star formation. Galaxies are believed

to migrate from the BC to the RS passing through a region with low number density of galaxies, known as the “Green Valley” (GV, Wyder et al. 2007). GV galaxies are considered a transitory population between the BC and RS (Salim et al. 2009). Galaxies in this region define this low number density “valley” because they are undergoing a rapid evolution phase, when their star-formation is being quenched (Crawford, Wirth & Bershadsky 2014).

The subject of transitional galaxy types has already been investigated for a few decades. For instance, some well known transitional objects are the post-starburst (“E+A”) galaxies (Dressler & Gunn 1983; Zabludoff et al. 1996; Tran et al. 2003; Goto 2005; Swinbank et al. 2012). and ultra-luminous infrared galaxies (Soifer et al. 1984; Caputi et al. 2006, 2009). More recently, several studies in the literature aim to investigate the properties and evolu-

* E-mail: plopes@astro.ufrj.br

tion of different transitional populations. [Wolf et al. \(2009\)](#) investigated the properties of optically passive spirals in the cluster A901/2; [Crossett et al. \(2014\)](#) investigated RS galaxies with residual star formation in massive nearby clusters; [McIntosh et al. \(2014\)](#) studied recently quenched elliptical galaxies (RQEs) in the local Universe; [Smethurst et al. \(2015\)](#) present evidence of different star formation histories of GV objects; and [Crawford, Wirth & Bershadsky \(2014\)](#) investigate the nature of GV and luminous compact blue galaxies (LCBGs) and their relation to BC and RS objects.

Galaxy stellar population properties also show a strong dependence on galaxy stellar mass ([Tortora et al. 2010](#); [Salim et al. 2009](#); [Guglielmo et al. 2015](#)). On average, high mass galaxies formed most of their stars at earlier epochs and in a much shorter time scale than lower mass systems. That effect is called downsizing ([Cowie et al. 1996](#); [Bundy et al. 2006](#); [Cimatti, Daddi & Renzini 2006](#); [Fontanot et al. 2009](#)). Disentangling the importance of environment and stellar mass, and even galaxy morphology, is a hard task. Currently, there is still a debate if the environmental dependence could simply be the result of different mass and/or morphological distributions with environment. In general, different studies indicate that both galaxy mass and environment are important. At least on what regards quenching, the environment is more relevant for lower mass objects ([Haines et al. 2007](#); [Vulcani et al. 2015](#)). In a recent study ([Guglielmo et al. 2015](#)) verify that current morphology is correlated to the star formation activity, but is not important for the stellar history. They also find the average star formation history (SFH) depends on galaxy mass, but at fixed mass the SFH depends on the environment.

This work is the fifth of a series aiming to investigate cluster and galaxies’ properties at low redshifts ($z \leq 0.1$). Our main goal is to study transitional galaxy populations characterizing their main properties in different environments, from the extreme field to the central parts of groups/clusters. For that purpose we separate our galaxy sample in four galaxy populations, two representing the “normal” galaxy bimodal distribution found in the local Universe, and two associated to intermediate types or galaxies in transition. In a similar way to what has been done by [Crawford, Wirth & Bershadsky \(2014\)](#) we simply consider photometric derived parameters for that separation. In our case, we use the (u-r) color and the concentration index ($C = R_{90}/R_{50}$). According to these parameters we separate the sample, calling the “normal” galaxies as “red bulges” and “blue discs”, and the transitional types as “red discs” and “blue bulges”. We compare several physical properties (such as age, metallicity, SFR, and stellar mass) of these four classes below, as well as their environmental variation from the field to clusters. The analysis is based on two complementary luminosity ranges ($M_r \leq M^* + 1$ and $M^* + 1 < M_r \leq M^* + 3$), where M^* is the characteristic magnitude of the luminosity function in the r -band.

This paper is organized as follows: §2 has the data description, where we also discuss the field sample, the local galaxy density estimates, the stellar population properties from different codes, visual morphologies, and the separation of the galaxy populations. In §3 we present the environmental variation of the transitional galaxy populations. In §4, to better characterize the samples, we compare physical properties and environmental parameters of the four

galaxy populations. In §5 we try to disentangle the importance of stellar mass and environment (local and global) for the galaxy populations. We also try to understand the nature of the transitional populations from their inspection in the $Z-M_*$, Age- M_* and sSFR- M_* planes, and the analysis of their star formation histories (SFH). In §6 we have a discussion on the quenching time of the “blue disc” population and on the nature of the transitional objects. We summarize our main results in §7. The cosmology assumed in this work considers $\Omega_m = 0.3$, $\Omega_\Lambda = 0.7$, and $H_0 = 100 \text{ h km s}^{-1} \text{ Mpc}^{-1}$, with h set to 0.7. For simplicity, in the following we are going to use the term “cluster” to refer loosely to groups and clusters of galaxies.

2 DATA

This work is based on photometric and spectroscopic data from the SDSS, as well as Wide-field Infrared Survey Explorer (WISE) photometry. In what follows we describe the cluster and field samples, and the main properties of the galaxy data we use.

2.1 Cluster sample

In the first paper of this series (hereafter paper I, [Lopes et al. 2009a](#)) we defined a cluster sample from the supplemental version of the Northern Sky Optical Cluster Survey (NoSOCS, [Lopes et al. 2004](#)). For that we used data from the 5th Sloan Digital Sky Survey (SDSS) release, from which we re-estimated photometric redshifts as in [Lopes \(2007\)](#). This sample comprises 7,414 systems well sampled in SDSS DR5 (details in paper I). NoSOCS has its origin on the digitized version of the Second Palomar Observatory Sky Survey (POSS-II; DPOSS, [Djorgovski et al. 2003](#)). In [Gal et al. \(2004\)](#) and [Odewahn et al. \(2004\)](#) the photometric calibration and object classification for DPOSS, respectively, are described. The supplemental version of NoSOCS ([Lopes et al. 2004](#)) goes deeper ($z \sim 0.5$), but covers a smaller region than the main NoSOCS catalog ([Gal et al. 2003, 2009](#)).

For a subset of the 7,414 NoSOCS systems with SDSS data we extracted a subsample of low redshift galaxy clusters ($z \leq 0.100$). This subsample comprises 127 clusters, for which we had enough spectra in SDSS for spectroscopic redshift determination, as well as to select cluster members and perform a virial analysis, obtaining estimates of velocity dispersion, physical radius and mass (σ_P , R_{500} , R_{200} , M_{500} and M_{200} ; details in paper I). This low-redshift sample was complemented with more massive systems from the Cluster Infall Regions in SDSS (CIRS) sample ([Rines & Diaferio 2006](#)). CIRS is a collection of $z \leq 0.100$ X-ray selected clusters overlapping the SDSS DR4 footprint. The same cluster parameters listed above were determined for these 56 CIRS clusters.

In the second paper of this series (hereafter paper II, [Lopes et al. 2009b](#)) we investigated the scaling relations of clusters using this combined sample of 183 clusters at $z \leq 0.100$, except for three systems that are not used for having biased values of σ_P and mass due to projection effects. For the clusters with at least five galaxy members within R_{200} we also have a substructure estimate, based on the DS, or

Δ test (Dressler & Shectman 1988). Details about this low-redshift sample and the estimates obtained for the clusters can be found in papers I and II.

The redshift limit of the sample ($z = 0.100$) is due to incompleteness in the SDSS spectroscopic survey for higher redshifts, where galaxies fainter than $M^* + 1$ are missed, biasing the dynamical analysis (see discussion in section 4.3 of Lopes et al. 2009a). We eliminated interlopers using the “shifting gapper” technique (Fadda et al. 1996), applied to all galaxies with spectra available within a maximum aperture of $2.50 \text{ h}^{-1} \text{ Mpc}$. We also estimated X-ray luminosity (L_X , using ROSAT All Sky Survey data), optical luminosity (L_{opt}) and richness (N_{gals} , Lopes et al. 2009a,b). The centroid of each NoSOCs cluster is a luminosity weighted estimate, which correlates well with the X-ray peak (see Lopes et al. 2006).

In Ribeiro et al. (2013) (hereafter paper III) we investigated the connection between galaxy evolution and the dynamical state of galaxy clusters, indicated by their velocity distributions. In Lopes, Ribeiro & Rembold (2014) (hereafter paper IV) we investigate the role of environment from the field, through the outer regions of clusters and their cores. In a forthcoming paper (Rembold, Ribeiro & Lopes) we will study the properties of brightest cluster galaxies and their connection to the parent clusters. Here we focus on the investigation of the properties of transitional galaxies (such as metallicity, L_{dust} , and star formation rate), and their relations with the environment and stellar mass. Note that for the cluster regions we only use galaxies that are selected as cluster members by the “shifting gapper” technique. A control field sample is described below.

In Lopes, Ribeiro & Rembold (2014) we implemented one modification to the “shifting gapper” technique, that resulted in the exclusion of a few lower mass systems (details in paper IV). Due to that our final sample comprises 152 groups and clusters, for which we have 6,415 galaxies, being 5,106 with $M_r \leq M^* + 1$ (from clusters at $z \leq 0.100$) and 1,309 galaxies with $M^* + 1 < M_r \leq M^* + 3$ (from objects at $z \leq 0.045$). Our clusters span the range $150 \lesssim \sigma_P \lesssim 950 \text{ km s}^{-1}$, or the equivalently in terms of mass, $10^{13} \lesssim M_{200} \lesssim 10^{15} M_\odot$. In that fourth paper we had investigated the role of environment beyond the extent of galaxy clusters, corroborating a scenario on which pre-processing in groups leads to a strong evolution in galaxy properties, before they are accreted by large clusters. This final galaxy sample, the cluster properties derived above, the density estimates and the field data, were all based on the SDSS DR7.

2.2 Field sample

The galaxy field sample is constructed as follows. From the whole DR7 data set we select galaxies that would not be associated to a group or cluster, considering the cluster catalog from Gal et al. (2009). To be conservative, we consider a galaxy to belong to the *field* if it is not found within 4.0 Mpc and not having a redshift offset smaller than 0.06 of any cluster from Gal et al. (2009). We select more than 60,000 field galaxies, but work with a smaller subset (randomly chosen) for which we derived local density estimates. In the end we use 2,936 field galaxies at $z \leq 0.100$ with $M_r \leq M^* + 1$, and 1,740 at $z \leq 0.045$ with $M^* + 1 < M_r \leq M^* + 3$ (the

same order of cluster galaxies). For these objects we compute density estimates (see below) in the same way as done for the cluster members.

Note this field sample is based on a comparison to one cluster catalog (Gal et al. 2009). As any other cluster catalog, the one from Gal et al. (2009) is complete for rich systems, but not for the smaller mass groups and clusters. Even if we were using all group and cluster catalogs available in the literature we would still be incomplete for low mass systems. Due to that we may select galaxies as field objects which may actually belong to small groups. Their local densities will then be high (see for instance Figs. 3 and 4 below, or Figs. 3 and 4 of Lopes, Ribeiro & Rembold 2014), with typical values $\text{Log } \Sigma_5 > 0$. However, the number of objects in this case is not large (as can be seen by the “scale” represented by the error bars in these figures), and we decided to leave them in the field sample, instead of making an arbitrary cut in Σ_5 . Another reason explaining these cases is the fact that we consider galaxies out to large distances from the clusters, so that some cluster galaxies have small local densities ($\text{Log } \Sigma_5 < 0.8$). The density overlap (between field and clusters results) we see in Figs. 3 and 4 happens for cluster galaxies that are in the infall (far from the center).

2.3 Local Galaxy Density Estimates

Considering the results from Muldrew et al. (2012) we decided to adopt a nearest neighbour method to estimate the local environment. The authors also mention that the choice of n - the rank of the density-defining neighbour - is very important, as the environment measure may loose power in the case n is larger than the number of galaxies residing in the halo. Hence, we chose to work with the Σ_5 local galaxy density estimator, as $n = 5$ is typically smaller than the number of galaxies we have per cluster and is a common estimate in the literature. To estimate local galaxy densities we proceed as follows. For every galaxy we compute its projected distance, d_5 , to the 5th nearest galaxy found around it, within a maximum velocity offset of 1000 km s^{-1} (relative to the velocity of the galaxy in question). The local density Σ_5 is simply given by $5/\pi d_5^2$, and is measured in units of galaxies/Mpc². Density estimates are also obtained relatively only to galaxies brighter than a fixed luminosity range, which we adopt as $M^* + 1.0$. On what regards the global environment we consider the distance to the center of the parent cluster, the cluster mass, or the comparison between field and cluster results.

2.3.1 Correction for the fiber collision issue

The fiber collision issue affects the SDSS spectroscopic sample and the derived density estimates. Due to a mechanical restriction spectroscopic fibers cannot be placed closer than 55 arcsecs on the sky. An algorithm used for target selection randomly chooses which galaxy gets a fiber, in case of a conflict (Strauss et al. 2002). This problem is reduced by spectroscopic plate overlaps, but fiber collisions still lead to a $\sim 6\%$ incompleteness in the main galaxy sample. Our approach to fix this problem is similar to the one adopted by Berlind et al. (2006) and La Barbera et al. (2010). For galaxies brighter than $r = 18$ with no redshifts we assume

the redshift of the nearest neighbour on the sky (generally the galaxy it collided with). This may result in some nearby galaxies to be placed at high redshift, artificially increasing their estimated luminosities. Due to that the collided galaxies also assume the magnitudes of their nearest neighbours, resulting in an unbiased luminosity distribution. Notice that the fraction of fixed galaxies is quite small (at most 6%, at highest densities); the above correction procedure has been shown to accurately match the multiplicity function of groups in mock catalogues (Berlind et al. 2006); and the velocity distribution (relative to group centre) of the original and fixed samples are consistent (La Barbera et al. 2010). Hence, the local galaxy density estimates take in account the fiber collision issue.

2.4 Absolute Magnitudes and Colors

For the current work we consider the stacked properties of cluster and field galaxies (in this case, regarding local density only). We do that considering the radial offset (in units of R_{200}), absolute magnitudes, colors and local densities of all member galaxies coming from the 152 clusters (or the field). Our sample consists of 5,106 bright member galaxies with $M_r \leq M^* + 1$ (at $z \leq 0.100$), 1,309 faint members with $M^* + 1 < M_r \leq M^* + 3$ (at $z \leq 0.045$), 2,936 bright field galaxies and 1,740 faint field galaxies. The bright and faint regimes are the same for cluster and field objects.

To compute the absolute magnitudes of each galaxy (in *ugri* bands) we consider the following formula: $M_x = m_x - DM - kcorr - Qz$ (x is one of the four SDSS bands we considered), where DM is the distance modulus (considering the redshift of each galaxy), $kcorr$ is the k -correction and Qz ($Q = -1.4$, Yee & López-Cruz 1999) is a mild evolutionary correction applied to the magnitudes (for each galaxy redshift). The k -corrections are obtained directly from the SDSS database, for every object in each band. Rest-frame colors are also derived for all objects. All the magnitudes we retrieved from the SDSS are de-reddened model magnitudes (see paper I).

2.5 The stellar population properties

A large number of galaxy properties were derived by different research groups for the SDSS data set. These parameters (such as stellar mass and star formation rate) are derived from spectral energy distribution (SED) fitting of stellar population synthesis models, considering the galaxy spectra or the broad band galaxy photometry. In the current work we consider parameters derived from the application of the STARLIGHT code (Cid Fernandes et al. 2005), the “Galspec” analysis provided by the MPA-JHU group (from the Max Planck Institute for Astrophysics and the Johns Hopkins University; Brinchmann et al. 2004), and the MAGPHYS code (da Cunha, Charlot & Elbaz 2008; da Cunha et al. 2013) applied to the SDSS plus WISE photometry (Chang et al. 2015). A brief description of the parameters we selected from these different methods is given below.

2.5.1 STARLIGHT

This code fits an observed spectrum with a linear combination of a number of template spectra with known properties (see paper III for details). We applied the code to the galaxy spectra of the galaxies in our sample. Among other parameters derived by STARLIGHT, we consider for this work the Age (and its dispersion) of the stellar population and the metallicity (Z). Both parameters (age and Z) represent the mass-weighted mean values. We have also derived a spectral classification, on which each object is called a Seyfert, LINER or Star-Forming (SF) according to their position in the Baldwin, Phillips & Terlevich (BPT) diagram. Galaxies with no significant emission lines are called passive. When applying STARLIGHT we require at least 30% of good spectral coverage (no bad quality flags on). Hence, we were not able to derive the above parameters for all galaxies in our sample. We end up with 5,060 bright member galaxies with $M_r \leq M^* + 1$ (at $z \leq 0.100$), 1,303 faint members with $M^* + 1 < M_r \leq M^* + 3$ (at $z \leq 0.045$), 2,912 bright field galaxies and 1,714 faint field galaxies. That represents $\sim 1\%$ loss.

2.5.2 MPA-JHU

The “galSpec” galaxy properties from MPA-JHU were derived for the DR8 galaxy spectra (nearly all of which were in DR7). The galaxy parameters we selected for this work are the BPT classification, the stellar mass and the star formation rate, and some index and line measurements, such as $D_n(4000)$ and $H\delta$. From the BPT diagram they divide galaxies into the “Star Forming”, “Composite”, “AGN”, “Low S/N Star Forming”, “Low S/N AGN”, and “Unclassifiable” categories. We consider the total stellar mass and star formation rate values (SFRs). The total stellar masses are based on model magnitudes. SFRs are computed within the galaxy fiber aperture using the nebular emission lines as described in Brinchmann et al. (2004). Outside of the fiber the estimates use the galaxy photometry, as in Salim et al. (2007). AGN and galaxies with weak emission lines, have SFRs estimates from the photometry. Due to the minimum criteria required by the MPA-JHU group (*e.g.*, redshift, S/N) not all galaxies in our sample are matched to the MPA-JHU results. Besides that we also require that the galaxies had the STARLIGHT parameters available. Hence, our sample with MPA-JHU values (common to the STARLIGHT) have 4,953 bright and 1,297 faint member galaxies, and also 2,864 bright and 1,672 faint field galaxies. That is 97% of the original sample.

2.5.3 MAGPHYS

Chang et al. (2015) combined SDSS and WISE photometry for the full SDSS spectroscopic galaxy sample, creating SEDs that cover $\lambda = 0.4 - 22 \mu m$. They used MAGPHYS to model simultaneously and consistently both the attenuated stellar SED and the dust emission at $12 \mu m$ and $22 \mu m$. We selected from their data the star formation rate, the stellar mass, the dust attenuation parameters μ and τ , as well as the dust, $12 \mu m$ and $22 \mu m$ luminosities. We were able to retrieve data from the catalog of Chang et al. (2015) for 4,900 bright and 1,244 faint member galaxies, and also

2,847 bright and 1,671 faint field galaxies. That is 97% of the original sample.

2.6 Transitional galaxy populations: Blue bulges and Red discs

Galaxies in the local Universe can generally be split in two types depending on their star formation activity and structure. Early-type galaxies are redder, with little star formation and high concentration. On the contrary late-type galaxies are bluer, show active star formation and are less concentrated. In paper IV we separate galaxies according to three parameters, two related to their star-formation properties ($u-r$ color and the spectral classification e_{class}), and one to the structure (the concentration index $C = R_{90}/R_{50}$). After Strateva et al. (2001) we called blue/red galaxies those with ($u-r$) values smaller/greater than 2.2. We considered objects with $C < 2.6$ as disc-dominated, and the rest as bulge-dominated galaxies ($C \geq 2.6$). Passive galaxies are those with e_{class} smaller than -0.05 , while the star-forming objects have larger values for this parameter. In that work we characterize the variation of different populations from the extreme field, through the outskirts of groups and clusters, up to the most dense regions of the Universe, the core of these structures. Our results indicate that pre-processing in groups leads to a strong evolution in galaxy properties, before they are accreted by large clusters. In agreement to Valentinuzzi et al. (2011), we find that local density is the main driver for galaxy evolution and not the parent halo mass. The evolution is such that star formation is quenched in the group scale, but morphological transformation is a separate process, occurring in larger galaxy systems.

In the current work we are interested on investigating the properties of transitional galaxies, and their environmental dependence. Those are likely objects caught in their way from the “blue cloud” to the “red sequence”, or in a few cases passive galaxies in a process of “rejuvenation”. We select these galaxies simply considering two of the parameters used in paper IV ($u-r$ and C). We define two types, which we call “red discs” (objects with $u-r \geq 2.2$ and $C < 2.6$), and “blue bulges” (with $u-r < 2.2$ and $C \geq 2.6$). Additionally we call the “regular” *early* and *late-types* as “red bulges” ($u-r \geq 2.2$ and $C \geq 2.6$), and “blue discs” (with $u-r < 2.2$ and $C < 2.6$), respectively. We compare the properties of these four classes below, as well as their variation from the field to clusters.

As we consider two simple parameters (an observed color and a concentration index) to separate galaxy populations there might be the question if the samples are largely affected by other populations. For instance, some of the “red discs” could be active star-forming galaxies that look red due to large amounts of dust. To verify that is not the case we inspect the color-color diagram, $(u-r)_0$ vs $(r-z)_0$, that is considered an effective way for separating passive from star-forming objects (Wuyts et al. 2007; Holden et al. 2012; Chang et al. 2015). Fig. 1 exhibits this diagram for the cluster galaxies considered in this work. Bright galaxies ($M_r \leq M^* + 1$) are in the left panels, while faint objects ($M^* + 1 < M_r \leq M^* + 3$) are in the right panels. On top we display red bulges (red points) and blue discs (blue points), while in the bottom panels we have red discs (black) and blue bulges (green). The thin lines represent the limits adopted

by Holden et al. (2012), and the thick lines shows the limits of Chang et al. (2015). Galaxies above (below) the lines are passive (star-forming) according to these different authors. We can see on all panels that galaxies we considered as quiescent/star-forming are generally above/below the division lines. In particular, the separation given by Chang et al. (2015) seems more effective. We also notice the “red discs” show only a small fraction of objects consistent to star-forming.

In Fig. 2 we confirm these conclusions through the inspection of the spectral classification from the STARLIGHT code (top) and the MPA-JHU group (middle panel). In the top panel a galaxy is called passive if there are no significant emission lines. From the BPT diagram an object is classified as Seyfert, LINER or Star-Forming (SF). In the middle panel a more detailed classification is given, with the “SF”, “Low S/N SF”, “Composite”, “AGN”, “Low S/N LINER” and “Unclassifiable” possibilities. Green lines are for “blue bulges”, blue lines for “blue discs”, black lines for “red discs”, and red lines for “red bulges”. These results consider all cluster galaxies with $M_r \leq M^* + 3$ (bright and faint). As we can see from the top panel $\sim 55\%$ of “red discs” are passive, with only $\sim 10\%$ being considered SF. The rest is most composed of LINERs. Similar conclusions are reached from the middle panel, with $< 10\%$ of the “red discs” being considered SF, although this more refined classification results in $\sim 25\%$ of these galaxies being called “Low S/N SF”.

In the bottom panel of Fig. 2 we display the Star Formation Rate (SFR) distribution estimated by the MPA group for these four populations. From this plot we can see the “red discs” are clearly distinct from the regular “blue discs”. However, the SFR distribution of the “red discs” is not identical to the “red bulges” neither. The former shown a non-negligible fraction of galaxies with residual SF in comparison to the latter. Note that the blue galaxies (bulges or discs) have more similar SFR distributions.

In order to have a rough idea of the morphological classification of the galaxies (especially the transition populations) we decided to perform a visual inspection of galaxies in our sample. That was done by BV for the “red disc” and “blue bulge” bright populations. A total of 1332 red discs were inspected, 836 within clusters and 496 in the field. For the blue bulge population we have 111 member galaxies and 157 field objects. The red discs were classified as “face-on red spiral” (*frs*), “face-on red/blue spiral” (*fbs*, with significant bluer colors in the arms), “edge-on disc” (*edg*), and “spheroidal” (*sph*). The blue bulges were classified as “spheroidal” (*sph*), “edge-on disc” (*edg*), “face-on disc” (*fd*), and “double core” (*dc*, for galaxies with two cores or strong signs of interaction). From these visual morphological classifications we verified that more than 50% of the “red discs” are classified as *frs* (“face-on red spiral”) and less than 20% are called *edg* (“edge-on disc”), reinforcing that misclassification due to edge-on spirals with high star formation is not an issue. The rest is classified as *fbs* ($\sim 10\%$) or *sph* ($\sim 20\%$). For the “blue bulges” more than 50% are classified as *sph* (“spheroidal”). The remaining objects are classified as *fd* ($\sim 35\%$), *edg* ($\sim 15\%$), or *dc* ($\sim 5\%$).

Note this classification process is very uncertain as even for the bright galaxies a high level of agreement between different classifiers is usually not achieved. That is due to the subjective nature of such visual inspection and low contrast

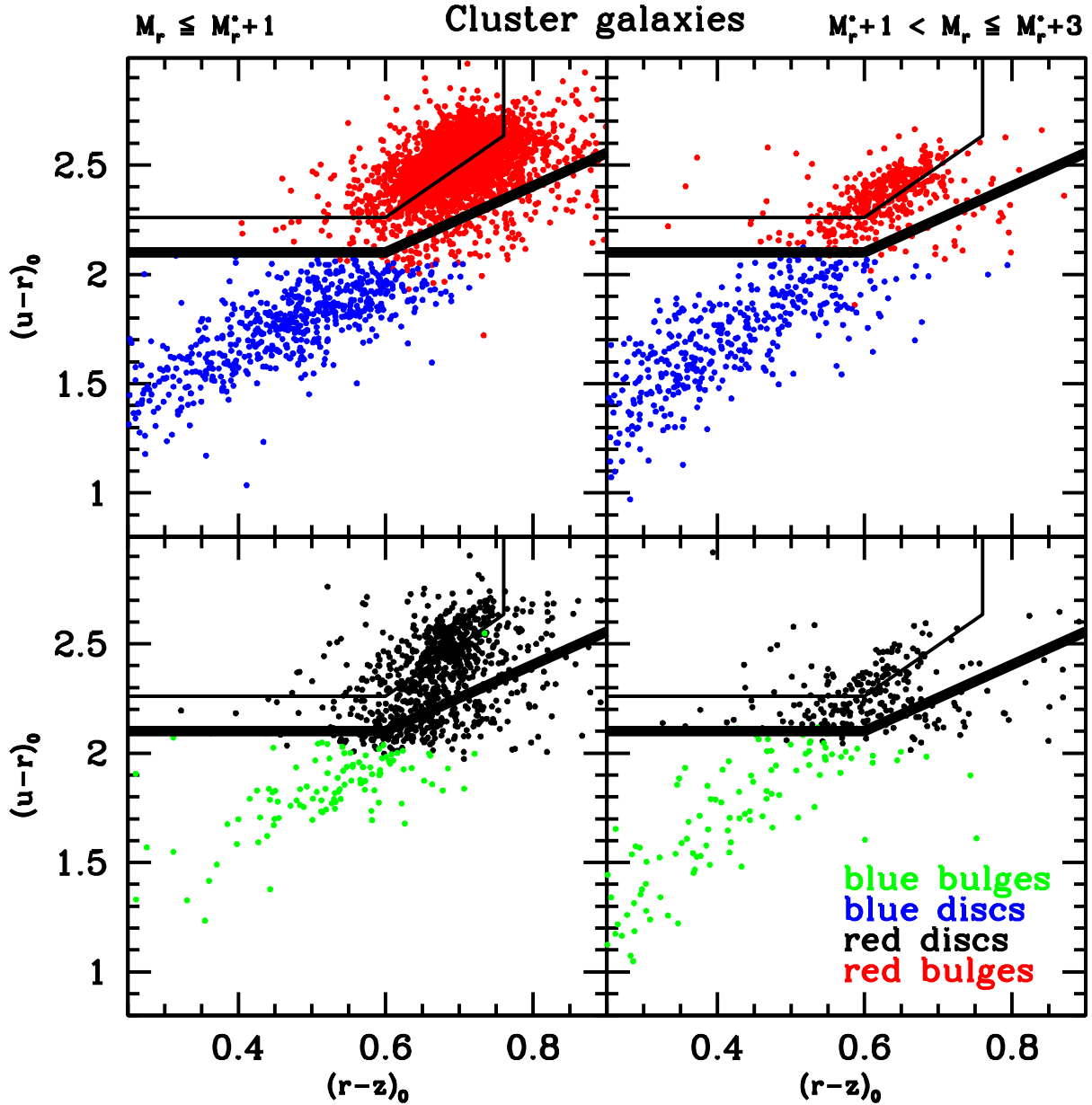


Figure 1. Color-color diagram showing bright galaxies ($M_r \leq M^* + 1$) in the left panels and faint objects ($M^* + 1 < M_r \leq M^* + 3$) in the right panels. Top panels show red bulges (red points) and blue discs (blue points). Bottom panels display red discs (black) and blue bulges (green). The thin lines show the limits adopted by Holden et al. (2012), while the thick lines shows the limits of Chang et al. (2015). Galaxies above (below) the lines are passive (star-forming) according to these different authors. Only cluster members are displayed, but the results are qualitatively the same for field galaxies. We can see on all panels that red (blue) galaxies are generally above (below) the division line from Chang et al. (2015).

of many stamps. Our main goal with such exercise was to confirm the expectations from Figs. 1 and 2, roughly verifying the “red discs” are not dominated by “edge-on discs” and the “blue bulges” are mostly classified as “spheroidal” systems. It is also important to mention the reason we did not extend such visual inspection for the fainter objects is the fact that even for some bright systems the classifica-

tion was already very difficult. As a matter of fact, our first step was trying to use the classification from the “Galaxy Zoo” project (Lintott et al. 2008), both for bright and faint galaxies of our sample. The “Galaxy Zoo” project considers an object as “spiral” if the debiased spiral fraction is larger than 0.8. If the debiased elliptical fraction is larger than 0.8 then the galaxy is classified as “elliptical”. If none of those

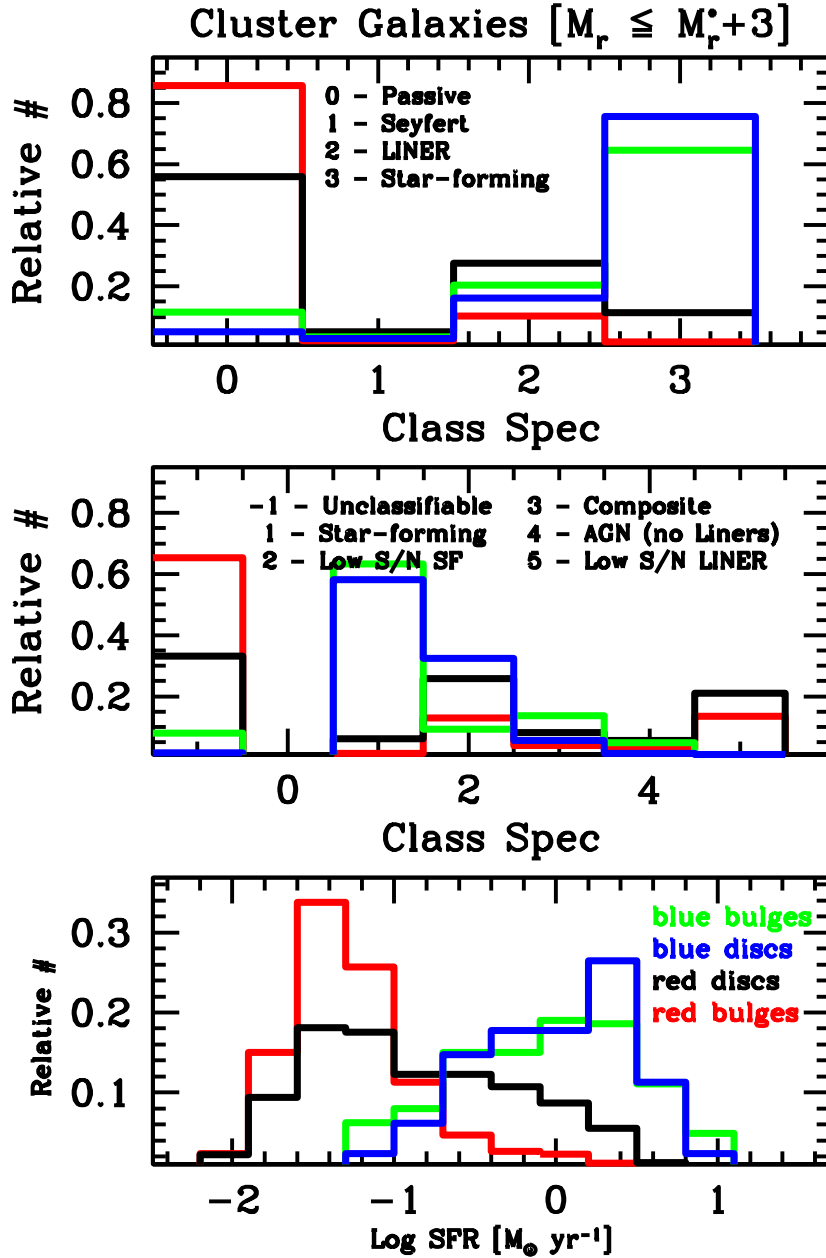


Figure 2. Top: spectral classification from STARLIGHT. We call a galaxy passive if there are no significant emission lines. An object is classified as Seyfert, LINER or Star-Forming (SF) according to their position in the BPT diagram; Middle: Similar to the top panel, but considering the BPT diagram of the MPA group; Bottom: Star Formation Rate (SFR) as estimated by the MPA group. Green lines are for “blue bulges”, blue lines for “blue discs”, black lines for “red discs”, and red lines for “red bulges”. All cluster objects with $M_r \leq M^* + 3$ (bright and faint) are considered. This figure shows that most “red discs” are passive, although having a non-negligible fraction of galaxies with residual SF compared to the “red bulges”. Most “blue bulges” are classified as SF objects and show similar SFR to the “blue discs”.

cases are true the galaxy is called “uncertain”. Considering those three possibilities we had to discard $\sim 60\%$ of our sample. Unfortunately, all these objects are called “uncertain”. Due to that we did not use the classification from “Galaxy Zoo”. It is important to stress that in the current work we are mainly interested on comparing the physical properties

and environment of galaxy populations divided by color and concentration, and not on performing a detailed morphological classification. Hence, we consider the morphological inspection we performed is satisfactory for our goals.

2.6.1 Possible systematic effects as a function of axial ratio

Although the “red disc” population seem not to be contaminated by a large number of highly elongated dusty spirals we decided to perform one more check based on the galaxy’s axial ratio (taking a/b as a proxy for inclination). As done by Masters et al. (2010) and Tojeiro et al. (2013) we consider an axial ratio limit of $\log(a/b) = 0.2$ to separate the low and high inclination objects. We compared a few physical properties (such as the sSFR) of disc galaxies with $\log(a/b) < 0.2$ and $\log(a/b) > 0.2$, doing so for the “red disc” and “blue disc” populations. We noticed the sSFR of low and high inclination “red discs” are indeed different, but the “blue discs” are not affected by a division in axial ratio. However, the two populations (red and blue discs) are still completely distinct. As we are most interested on investigating the differences between red and blue discs, we decided not to impose an axial ratio cut to our sample. We found this cut on axial ratio does not affect any of our results and conclusions through the paper. For instance, the comparison of “blue discs” and “red discs” in Fig. 13 (showing the relations between stellar metallicity, the age of the stellar population, and the sSFR *vs* stellar mass) is not affected by a restriction to galaxies with $\log(a/b) < 0.2$. Hence, as the environmental variation of the populations or their differences are not sensitive to an axial ratio cut we did not impose such restriction to our sample.

3 THE ENVIRONMENTAL VARIATION OF TRANSITIONAL GALAXY POPULATIONS

In this section we investigate the variation of the two transitional galaxy populations (“red discs” and “blue bulges”) with the environment, characterized by the local galaxy density, and the normalized radial distance to the parent cluster. We have also investigated the environmental influence in different ranges of galaxy stellar mass. We show the variation of these populations at fixed morphology. For instance, we verify how the fraction of “red discs” relative to all discs depends on environment (as well as the fraction of “blue bulges” relative to all bulges).

3.1 Variation with Local Galaxy Density

In Figs. 3 and 4 we show the variation in the number of “red discs” over all discs (top), and “blue bulges” relative to all bulges (bottom), as a function of local galaxy density (Σ_5). Fig. 3 is for bright galaxies ($M_r \leq M^* + 1$) and Fig. 4 for faint objects ($M^* + 1 < M_r \leq M^* + 3$). Red open circles show cluster members, while blue filled circles indicate field galaxies. From the low to the high density regime the number of “blue bulges” (relative to all bulges) decreases, especially once within clusters. That is true for bright and faint objects. For the “red discs” we detect a nearly flat relation for field galaxies and a steep increase in the relative number to the disc population, both for bright and faint objects. The number of “blue bulges” over bulges varies from $\sim 1\%$ to $\sim 18\%$ (for bright galaxies), and from $\sim 10\%$ to $\sim 50\%$ (for faint objects). The number of “red discs” over

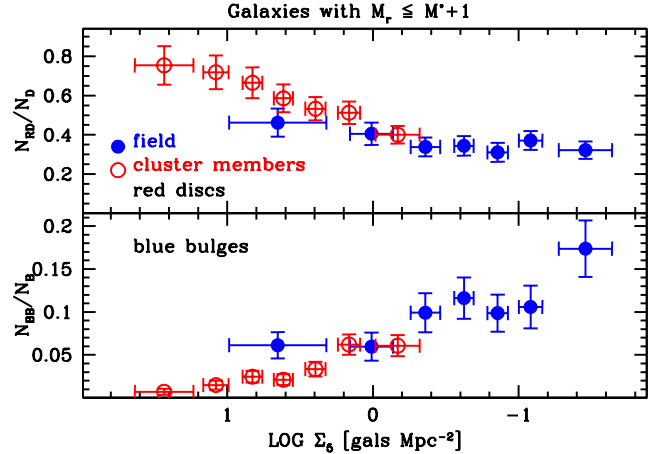


Figure 3. Fraction of red discs (top) relative to the full disc population, and the fraction of blue bulges (bottom) relative to all bulges. Both fractions are displayed as a function of local galaxy density (Σ_5). These results consider bright galaxies ($M_r \leq M^* + 1$) only. At fixed morphology, from low to high density the proportion of “blue bulges” decreases. For the “red discs” the relation is nearly flat in the field, increasing steeply in the cluster domain.

discs changes from $\sim 35\%$ to $\sim 80\%$ (for the bright regime), and from $\sim 3\%$ to $\sim 60\%$ (for faint galaxies).

A result we should highlight is the fact disc galaxies become redder as density increases, but this effect is mainly seen in the cluster environment. In particular, as we are going to see below (Figs. 5 and 6), this transformation occurs mainly within the cluster virial radius. That is another way to represent the colour-density (or colour-radius) relation. At fixed morphology (“discs”) we detect a steep variation in the number of “red discs” over all “discs” with density (once within the clusters). Hence, those “blue discs” change their colour - becoming red - while still keeping the same morphology.

3.2 Dependence on the Cluster Radial Distance

In Figs. 5 and 6 we show the variation in the number of “red discs” over all discs (top), and “blue bulges” relative to all bulges (bottom), as a function of the normalized distance to the parent cluster (R/R_{200}). The results are only shown to cluster members. Fig. 5 is for bright galaxies ($M_r \leq M^* + 1$) and Fig. 6 for faint objects ($M^* + 1 < M_r \leq M^* + 3$). The symbols are the same as in Figs. 3 and 4, for cluster galaxies. From the outskirts to the inner parts of the clusters we see the two populations (“blue bulges” and “red discs”) are nearly constant until within R_{200} , and then the relative numbers decrease (increase) for the “blue bulges” (“red discs”) all the way to the core. That is true for bright and faint galaxies. These results reinforce the relevance of the

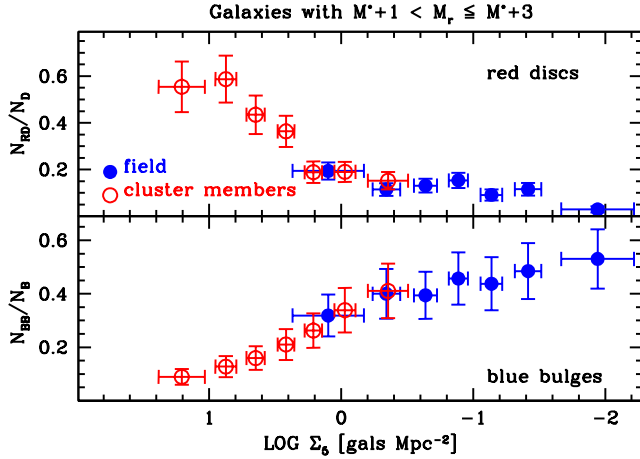


Figure 4. Analogous to Fig. 3, but showing the results for faint galaxies ($M^* + 1 < M_r \leq M^* + 3$) only. These two figures represent the colour-density relation, showing that at fixed morphology (discs) the proportion of red galaxies increases with density.

cluster environment on transforming galaxy properties, especially those related to the star formation activity.

3.3 Dependence on the Galaxy Stellar Mass

In Fig. 7 we show again the variation in the number of “red discs” over all discs (top), and “blue bulges” relative to all bulges (bottom), as a function of the local galaxy density (Σ_5). This figure is analogous to Fig. 3, but now we show the results for bright and faint galaxies at the same time ($M_r \leq M^* + 3$), as we consider four different stellar mass ranges: $\text{Log} M_* \leq 10.3$ (circles), $10.3 < \text{Log} M_* \leq 10.6$ (squares), $10.6 < \text{Log} M_* \leq 10.9$ (triangles), and $\text{Log} M_* > 10.9$ (hexagons). From low to high stellar mass the line used in Fig. 7 is progressively thicker. Cluster members are shown in red (filled symbols), while field galaxies are in blue (open symbols).

As expected, the largest fractions of red galaxies are seen for the higher mass galaxies (the last two mass bins, $\text{Log} M_* > 10.6$). However, the dependence on Σ_5 is smaller for these massive galaxies when compared to the first two mass bins ($\text{Log} M_* \leq 10.6$), for which we see a steep increase in the number of “red discs” over discs, especially within clusters. On what regards the “blue bulges” the variation with Σ_5 is significant only for the lowest mass galaxies ($\text{Log} M_* \leq 10.3$). These results reinforce the idea that star formation is halted first in higher mass galaxies. The fact the massive field “red discs” have a negligible variation with local density, but their cluster counterpart still depend on Σ_5 (increasing from $\sim 80\%$ to $\sim 100\%$) stress the importance of the cluster environment to transform these objects.

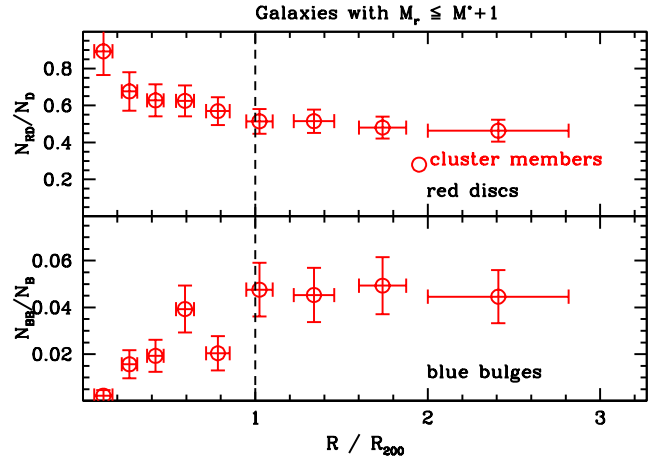


Figure 5. Fraction of red discs (top) and blue bulges (bottom) as a function of the normalized distance to the cluster center (R/R_{200}). Only cluster members are shown. These results consider bright galaxies ($M_r \leq M^* + 1$) and the fractions are relative to the full disc population (top), and to all bulges (bottom). The vertical dashed line indicates the R_{200} radius. From the outskirts to the inner parts of the clusters a large variation is seen only once within the virial radius (approximated by R_{200}).

4 ENVIRONMENTAL AND PHYSICAL PROPERTIES OF THE GALAXY POPULATIONS

In this section we compare some physical properties (such as age and metallicity) of the four galaxy populations defined for this work (“blue bulges”, “blue discs”, “red discs” and “red bulges”), as well as some properties related to the environment (R/R_{200} , crossing time, and Σ_5). This comparison is made with the help of the cumulative distributions of these properties. Our goal is to verify if the galaxy populations can really be considered as different types of objects or, in other words, systems at different evolutionary stages. The crossing time (t_{cross}) is defined as the distance of the galaxy to the group center divided by the group’s line-of-sight velocity dispersion. For a large sample of galaxies t_{cross} provides a measure of how long galaxies have been affected by the group environment (Lackner & Gunn 2013).

Fig. 8 shows the cumulative distributions of these four populations, with “blue bulges” in green, “blue discs” in blue, “red discs” in black, and “red bulges” in red (as in Fig. 2). The normalized distance to the cluster center (R/R_{200}) is exhibited on top, the crossing time (shown in units of Hubble time) is in the middle panel, and Σ_5 is in the bottom panel. Only bright cluster galaxies ($M_r \leq M^* + 1$) are considered. We can see there is little difference in the typical environment of red galaxies (discs and bulges). The same can be said for the blue objects. However, at fixed morphology we see clear differences between red and blue discs, as

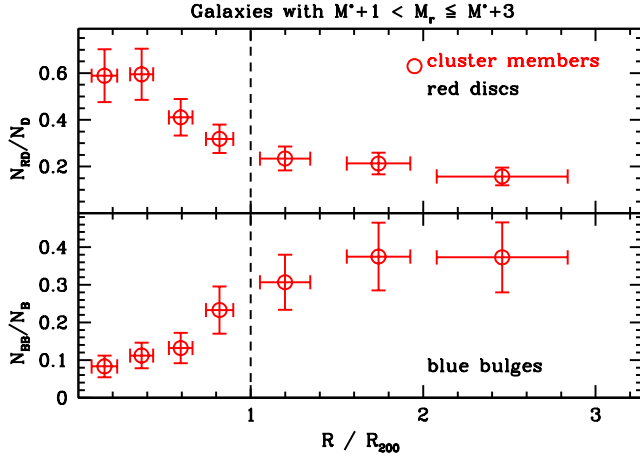


Figure 6. Same as previous figure, but showing results for faint galaxies ($M^* + 1 < M_r \leq M^* + 3$). From the outskirts to the center of clusters the relative numbers of the two populations (“blue bulges” and “red discs”) change mostly once within R_{200} . These results reinforce the importance of the cluster environment to transform galaxy properties.

well as bulges. As it is well known red objects are generally found at the highest densities, in the central parts of clusters, and have shorter crossing times than blue galaxies. As we see from Fig. 8 red and blue discs are located in very different environments, reinforcing the idea these two populations are different. Hence, as we suggested above, the “red disc” population is not simply the result of contamination of disc galaxies that look redder due to dust emission.

Fig. 9 is analogous to Fig. 8, but shows the cumulative distributions of the age of the stellar population (top), the stellar metallicity (Z) in the middle panel, and the stellar mass (bottom panel). The color codes are the same as in Fig. 2 and will be kept for future plots from now on. As above only bright cluster galaxies are shown. We see a large difference in these physical properties of galaxies at fixed morphology (red and blue discs, or bulges). However, we also see a significant difference in the properties of red galaxies (discs and bulges), especially for the two top panels (age and metallicity). Hence, despite the fact these objects are found at similar environments (see Fig. 8) they have different ages and metallicities. “Red bulges” have an older stellar population and higher metallicities than “red discs”. The stellar masses of the former are also slightly higher than the latter.

Another feature we detect in Fig. 9 is the metallicity difference between blue discs and bulges. Although, these two populations are found in similar environments and have similar age distributions the “blue bulges” display higher Z values than the “blue discs”, and actually get close to the results for the “red discs”. Part of this effect is explained by the slightly larger masses of the “blue bulges”. But the main

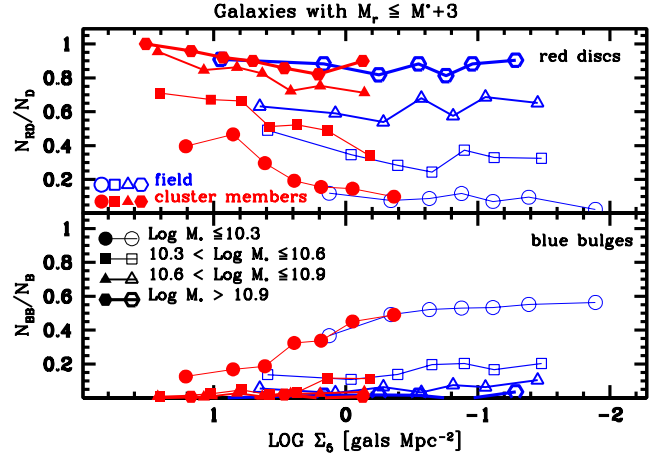


Figure 7. Same as in Fig. 3, but splitting the sample according to the galaxy stellar mass. We consider four intervals: $\text{Log} M_* \leq 10.3$, $10.3 < \text{Log} M_* \leq 10.6$, $10.6 < \text{Log} M_* \leq 10.9$, $\text{Log} M_* > 10.9$. From low to high stellar mass the line used to connect the points is progressively thicker. As before, cluster members results are in red and field results in blue. All galaxies with $M_r \leq M^* + 3$ (bright and faint) are considered. We can see that star formation is halted first in higher mass galaxies. For the “red discs” the largest variation is seen for the lower mass objects ($\text{Log} M_* \leq 10.6$), while for the “blue bulges” a significant change is detected only for the lowest mass galaxies ($\text{Log} M_* \leq 10.3$).

reason is environmental. Fig. 9 shows the results only for bright cluster galaxies. For the field data we find the metallicity distributions of blue discs and bulges to be consistent to each other, and different than the Z values of red galaxies. The same is true if we also include the fainter galaxies. This environmental difference may be related to different types of galaxies composing the “blue bulge” population in the clusters compared to the field. In §5.3 we investigate asymmetry in the “blue bulge” population. From the asymmetry distribution and visual inspection we find that the “blue bulges” can be simple spheroids, or bulge dominated low mass spirals, or wet mergers. We believe that different fractions of these types (among the “blue bulges”) can explain the metallicity difference between “blue bulges” in the field and clusters. Further investigations are left for future work.

The age, metallicity, stellar mass and SFR displayed in Figs. 9 and 2 were derived from STARLIGHT and the MPA-JHU group (based only on SDSS data). Now we investigate the results obtained with parameters derived from the MAGPHYS code applied to SDSS plus WISE data. Fig. 10 is analogous to Fig. 9, but exhibiting the $12\mu\text{m}$ luminosity divided by stellar mass (top), the dust luminosity divided by mass (middle) and the stellar mass (bottom). All cluster galaxies ($M_r \leq M^* + 3$) are considered. From the bottom panel we can see the stellar mass distributions are

very similar to the ones derived from the MPA-JHU group (Fig. 9), but now considering the faint regime. As noticed by Chang et al. (2015) adding the four WISE bands do not lead to different stellar masses estimates. However, they verify the SFR estimates are very different. We decided not to perform this comparison in the current work. However, we can say that when also using WISE data the SFR values become larger for the star-forming (blue galaxies), and smaller for the passive objects (red galaxies). The central panel of Fig. 10 shows that “blue bulges” have similar dust luminosities than “blue discs”, and the latter have much larger L_{dust} values than “red discs”. The “red bulges” have even lower luminosities. The top panel of this figure reinforces what is seen in the bottom panel of Fig. 2. As the $12\mu m$ luminosity is a good SFR indicator (Chang et al. 2015) we can see the most luminous galaxies in this band are the blue ones, while the less luminous are the red galaxies (with the “red bulges” being the less luminous of all). Hence, the $12\mu m$ luminosity indicates a high star formation rate for the two blue populations (bulges and discs), while still pointing to a residual star formation for the “red discs”.

5 ROLE OF STELLAR MASS, LOCAL AND GLOBAL ENVIRONMENT

We now want to disentangle the impact of the galaxy stellar mass and the environment (local and global) for the physical properties of the different galaxy populations.

First we show in Fig. 11 the cumulative distributions of the specific star formation rate (sSFR) in different ranges of local galaxy density. Each galaxy population (“blue bulges”, “blue discs”, “red discs” and “red bulges”) is divided in five ranges of galaxy density, with the same number of objects. However, to avoid confusion, we exhibit only the lower (dashed) and upper density (solid) cumulative distributions, for each population. In the top panel we present the results for cluster galaxies and in the bottom panel for the field. Doing so we can assess the importance of the local environment (through the local galaxy density) and the global environment (comparing field and cluster results). For this plot all galaxies with $M_r \leq M^* + 3$ are considered.

We can derive a few interesting conclusions from this figure. First the blue and red populations do not overlap. Second, the “red discs” and “red bulges” are distinct objects both at low and high local density values. Even the highest density results for the “red discs” do not overlap the lower density curve of “red bulges”. Third, the blue objects show similar distributions, with the “blue discs” being insensitive to local environment, and the “blue bulges” displaying different distributions with local density. However, the largest variations with local density are seen for the red objects at fixed morphology, especially for the “red discs” in the cluster environment. Four, the comparison of field and cluster results show no significant variation, except for the red objects distributions at high Σ_5 (solid curves).

As a comparison we show in Fig. 12 the cumulative distributions of the specific star formation rate (sSFR), but now in different ranges of stellar mass. As before, all galaxies with $M_r \leq M^* + 3$ are considered. Each of the four galaxy populations is divided in five ranges of stellar mass, with the same number of objects. However, we show only the lower

(dashed) and upper mass (solid) cumulative distributions. In the top panel we show cluster results, while in the bottom we display the field distributions. Some results are similar to what is seen in Fig. 11. For instance, the blue and red populations show distinct distributions, both in the field and clusters. However, now we see that all the four populations depend on stellar mass and this dependence is larger than what has been seen for local density. Even the two blue populations show large differences for low and high stellar mass. As a function of stellar mass we can now see differences in the field and cluster distributions when inspecting each of the four galaxy populations. However, as before the largest variation is seen for the highest mass bin (solid curves) of the “red discs”, indicating that as these galaxies move from the field to clusters (and increase in mass) their star formation rate (SFR) decreases.

From these two figures we can infer that both the local and global environment affect the sSFR, but the former may be more important. However, the most effective parameter to all the four galaxy populations is the stellar mass, both in the field and clusters.

We have also performed a similar analysis considering the $D_n(4000)$ parameter that traces evolved stellar populations (> 1 Gyr, Kauffmann et al. 2004; Chang et al. 2015). The $D_n(4000)$ distributions show similar behaviour to the sSFR ones, reinforcing that stellar mass is the most effective parameter affecting all four populations, with the red discs being the most sensitive one. Other parameters, such as $H\delta$ (traces the presence of young stellar populations, < 1 Gyr), L_{dust} and Z lead us to similar conclusions.

5.1 From Blue to Red Discs Across Different Environments

The study of the variation of galaxy populations (traced by morphological or star-formation indicators) with environment can be used to constrain galaxy formation and evolution, and in particular, to understand the mechanisms responsible for quenching star formation. For instance, the variation of the star-forming or blue fractions with X-ray luminosity (analogous to the relations shown in §3) can be used as evidence in favor (or not) of the *ram-pressure stripping* effect (see Lopes, Ribeiro & Rembold 2014; Roberts et al. 2016).

We can also use relations between different galaxy parameters for that purpose. In the current work, if we assume the “red discs” to originate in the blue cloud, being a transition population to the red sequence, it is interesting to compare the location of blue and red discs in different parameter spaces.

Some of these correlations (e.g., $Z-M_*$) are also useful to probe different scenarios for transforming galaxies and quench their star formation. As recently proposed by Peng et al. (2015) the relation between stellar metallicity and stellar mass is an important tool to probe which mechanism is more relevant to quench galaxies. What is actually used is the metallicity difference between star-forming and passive populations. Rapid quenching (*strong outflows or ram-pressure stripping*) with sudden removal of the gas reservoir of the galaxy would imply in small metallicity differences between different galaxy populations. In the slow quenching scenario, through *strangulation*, the galaxy would

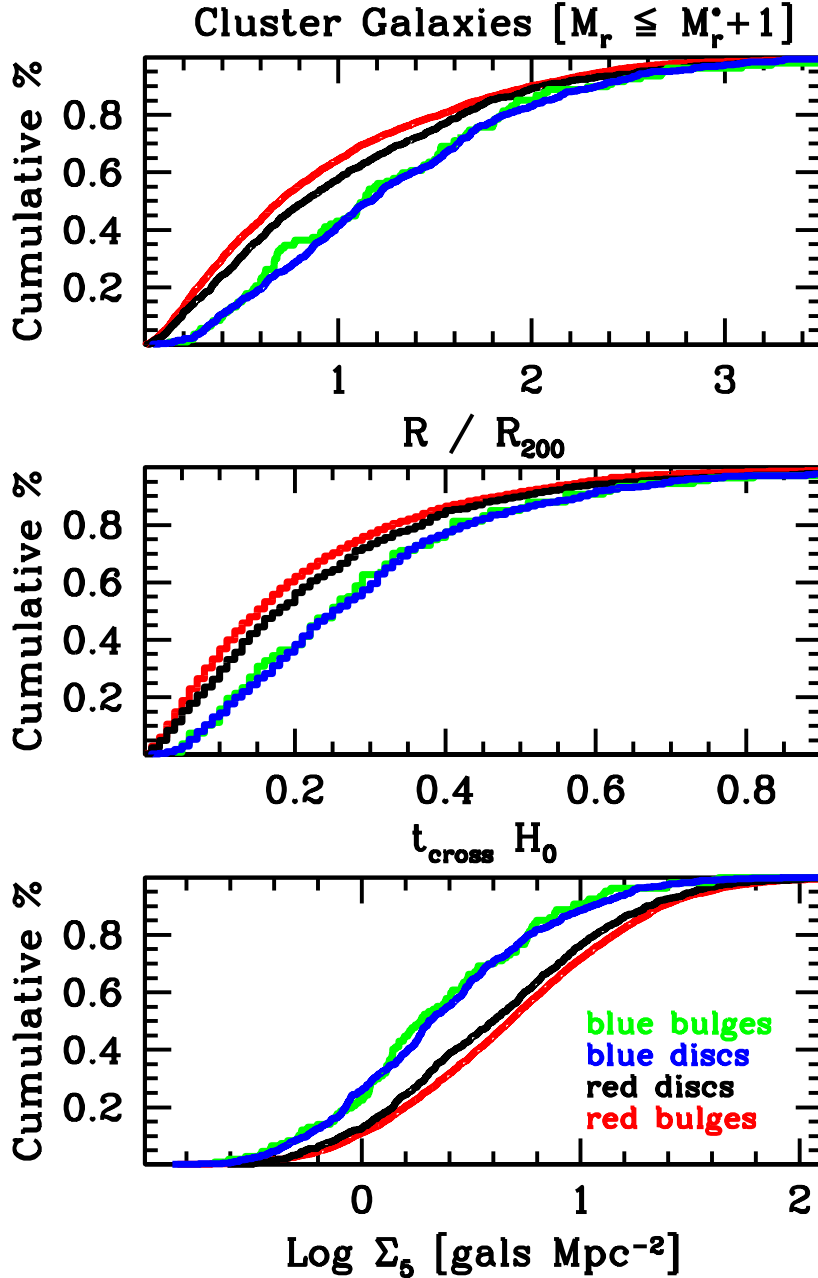


Figure 8. Cumulative distributions for different galaxy populations: “blue bulges” in green, “blue discs” in blue, “red discs” in black, and “red bulges” in red. The top panel shows the normalized distance to the cluster center (R/R_{200}), while the middle panel displays the crossing time, and the local galaxy density is exhibited in the bottom panel. Only bright cluster galaxies ($M_r \leq M_r^* + 1$) are considered. At fixed morphology red and blue discs are found in different environments (the same is true for the bulges, red and blue). On the contrary, at fixed color the galaxy environment is similar, for bulges or discs.

still form stars for a long period with its surviving gas content. Until it is exhausted metallicity would still grow, implying in large differences between passive and star-forming objects (see Peng et al. 2015; Roberts et al. 2016).

With that in mind we plot in Fig. 13 the relations between stellar metallicity (Z), the age of the stellar population, and the sSFR *vs* stellar mass, for the “blue discs” (blue points) and “red discs” (black points). We also discriminate

between field (open symbols) and cluster (filled symbols) results. The error bars indicate the 1σ standard error on the biweight location estimate. In the top panel we display the relation with Z , while age is shown in the middle and sSFR in the bottom panel. We can see a clear difference in the top panel results for red and blue discs, especially for lower masses. Note also that “blue discs” extend to a lower mass regime, while the opposite is true for the “red discs”.

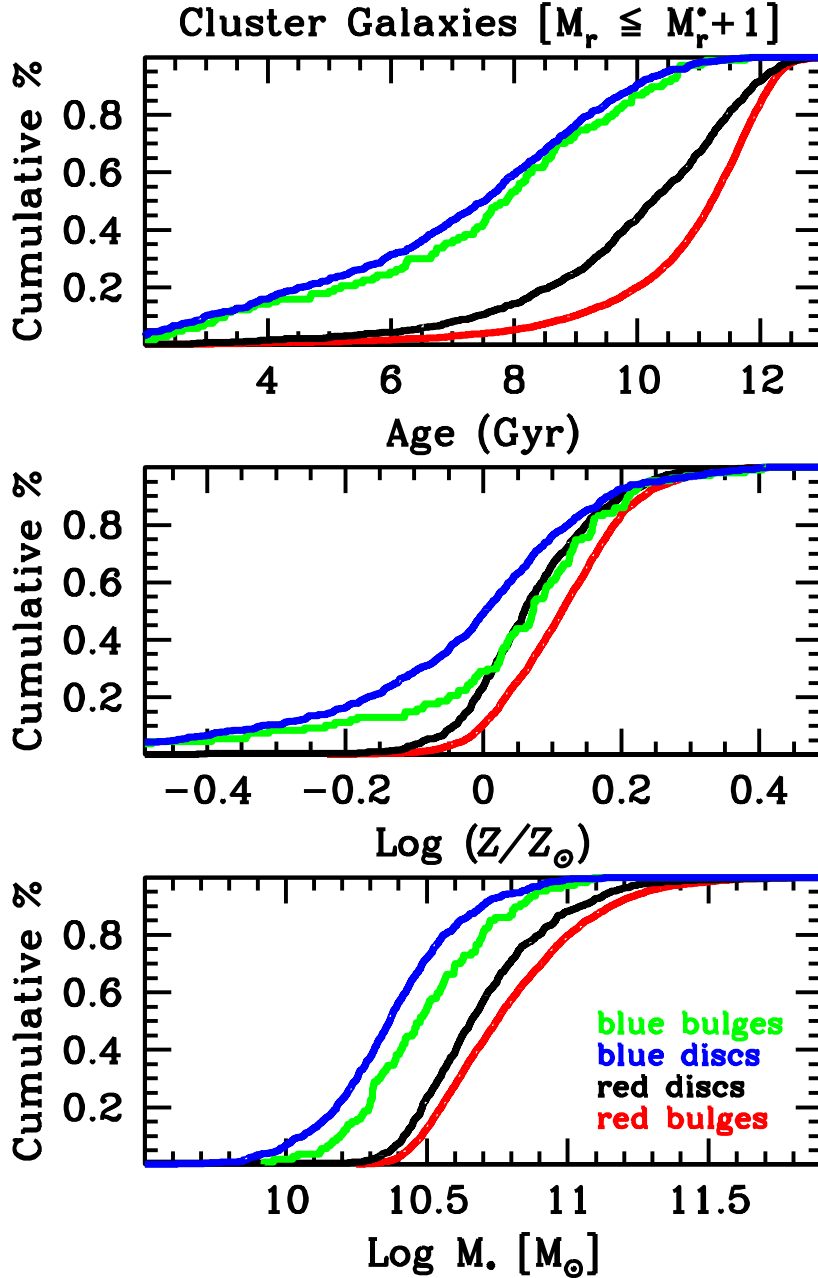


Figure 9. Analogous to the previous figure, but showing the age of the stellar population (top), the metallicity (middle) and the stellar mass (bottom). Only bright cluster galaxies ($M_r \leq M_* + 1$) are considered. The color codes are the same as in the previous figure. At fixed morphology we detect a large difference in these physical properties. Hence, red and blue discs (or bulges) can be considered as distinct populations.

We also detect a small difference between field and cluster for low mass “blue discs” ($\text{Log } M_* \sim 9.5$, in the top panel) and for massive “red discs” ($\text{Log } M_* > 10.5$, in the bottom panel).

The metallicity difference between “red discs” and “blue discs”, in the top panel of Fig. 13, is seen both in the field and in clusters. An interesting feature is the fact the differences are slightly larger for field galaxies than cluster objects. The metallicity difference at $\text{Log } M_* = 9.5$ is ~ 0.22 dex for the

field and ~ 0.14 dex for cluster galaxies. These values decrease steeply for $\text{Log } M_* \sim 10$. Comparing these results to the right panel of Figure 2 from Peng et al. (2015) we would estimate that field “red discs” are observed around 2–3 Gyr after quenching due to strangulation, with the time scale for cluster galaxies being ~ 2 Gyr. The different time scale between field and cluster galaxies could indicate the importance of the cluster environment to accelerate galaxy quenching. Mechanisms such as *ram-pressure strip-*

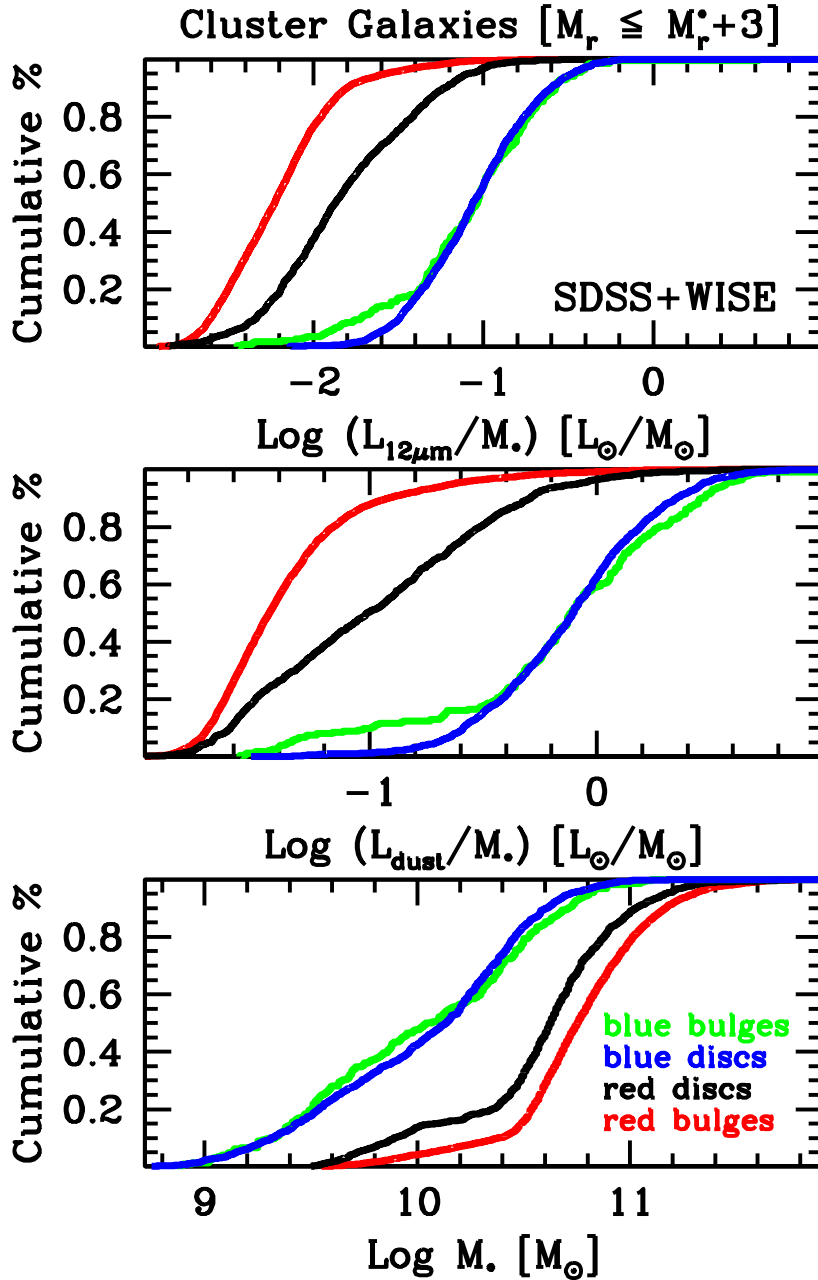


Figure 10. Analogous to Fig. 9, but showing the results derived from the MAGPHYS code applied to SDSS+WISE data. We exhibit the $12\mu\text{m}$ luminosity divided by stellar mass (top), the dust luminosity divided by mass (middle) and the stellar mass (bottom). All cluster galaxies ($M_r \leq M^* + 3$) are considered. The color codes are the same as in Fig. 9. The $12\mu\text{m}$ and dust luminosities point to higher star formation values for the two blue populations, but still indicates a residual star formation for the “red discs”.

ping (common in the cluster cores) could add up to the strangulation process, resulting in a shorter time scale for galaxies to halt star formation. In the middle panel of Fig. 13 we also detect an approximately constant age difference, with stellar mass, of ~ 2 Gyr between the two populations. However, a proper comparison of the time scales inferred from the metallicity and age differences would require a detailed analysis of the SFR, which is beyond the scope of this work.

It is important to emphasize the comparison we make

is not between a star-forming galaxy population and a truly passive population, as we still have residual star formation among the “red discs”. If we would isolate only the SF “blue discs” (from the BPT diagram) and the passive “red discs” the differences we obtain would be larger, closer to those from Peng et al. (2015) and Roberts et al. (2016). However, we decided to show the results as in Fig. 13 as we assume “red discs” to be a transition population between “blue discs”

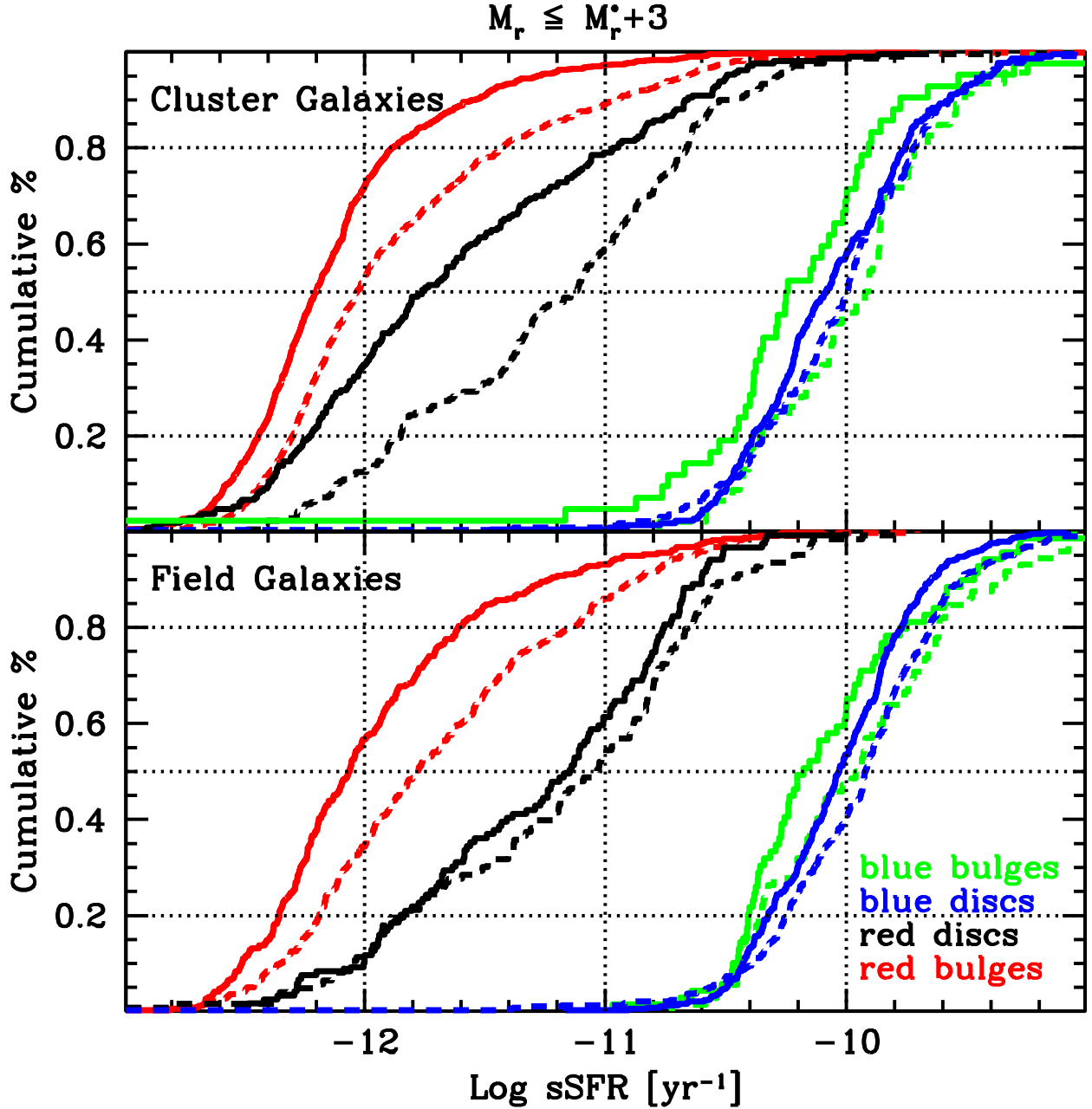


Figure 11. Analogous to Fig. 9, but showing the results only for the specific star formation rate, and in different local galaxy density bins. Each galaxy population (“blue bulges”, “blue discs”, “red discs” and “red bulges”) is divided in five ranges of galaxy density, with the same number of objects. However, to avoid confusion, we only exhibit the lower (dashed) and upper density (solid) cumulative distributions, for each population. Results for cluster galaxies are shown in the top panel, and for the field in the bottom panel. For this figure all galaxies with $M_r \leq M^* + 3$ (bright and faint) are considered. The color codes are the same as in Fig. 9. From this figure we conclude the blue and red populations do not overlap; “red discs” and “red bulges” are distinct objects; the blue objects display similar distributions; the largest variations with local density (at fixed morphology) are found for the red objects; and field and cluster results show no large differences (except for the red objects at high density).

and “red bulges”. It is encouraging to detect such metallicity differences between the populations we show.

The difference between field and cluster for massive “red discs” ($\text{Log } M_* > 10.5$), seen in the bottom panel of Fig. 13, motivated us to investigate further the dependence of the

“red disc” population in the $\text{sSFR}-M_*$ plane for different environments. First we consider only cluster members, in order to verify how these galaxies are affected when being accreted by clusters. To do so we show in Fig. 14 the $\text{sSFR}-M_*$ relation for “red discs”, dividing the results in four

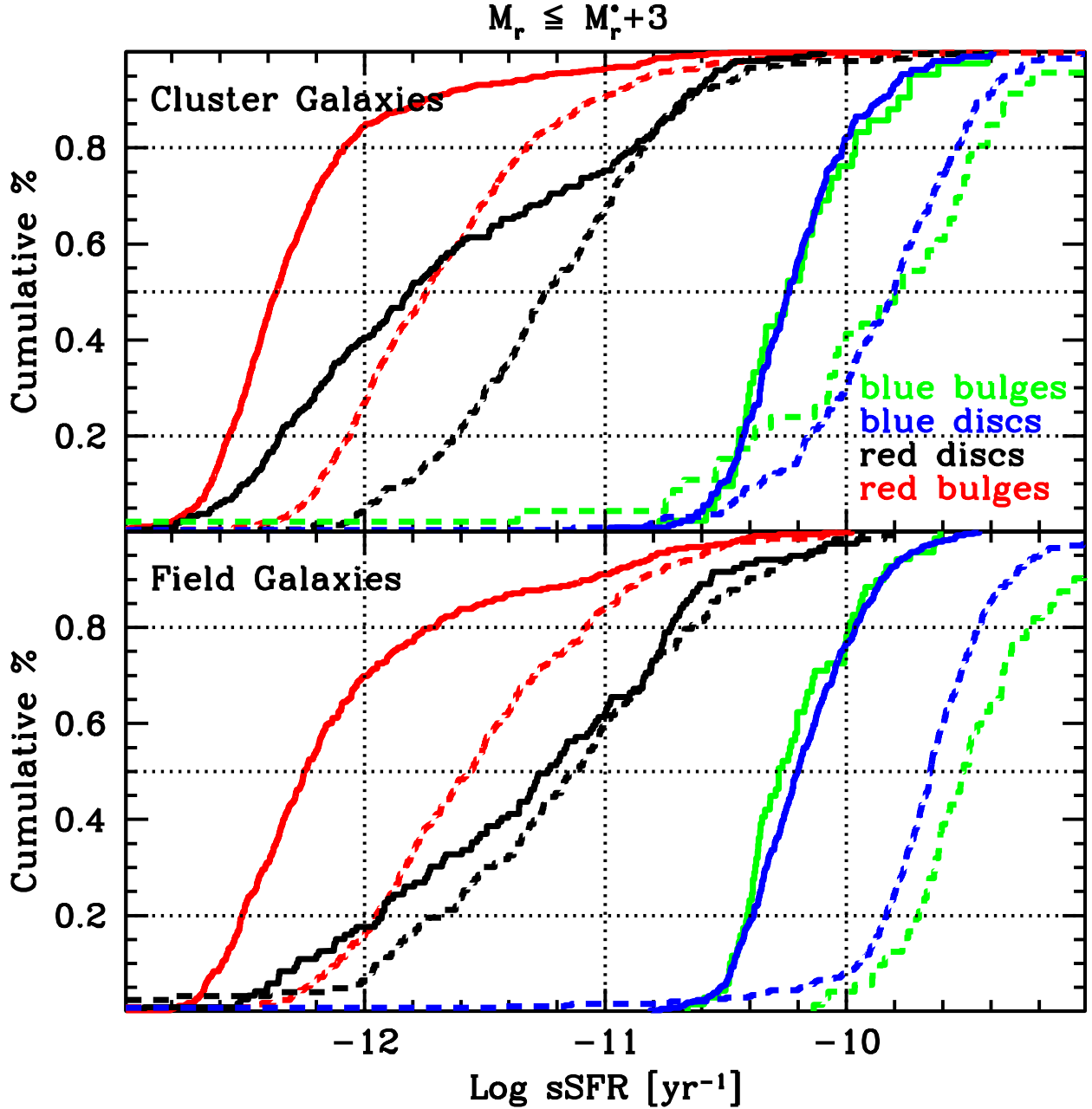


Figure 12. Analogous to the previous figure, but showing the results for different stellar mass bins. Each galaxy population (“blue bulges”, “blue discs”, “red discs” and “red bulges”) is divided in five ranges of stellar mass, with the same number of objects. However, we only exhibit the lower (dashed) and upper mass (solid) cumulative distributions for each population. Results for cluster galaxies are shown in the top panel, and for the field in the bottom panel. For this figure all galaxies with $M_r \leq M_r^* + 3$ (bright and faint) are considered. The color codes are the same as in Fig. 9. All the four populations show a strong dependence on stellar mass (larger than what has been seen for local density). Hence, the most important parameter affecting all the four galaxy populations is the stellar mass, both in the field and clusters.

ranges of the phase-space parameter $(R/R_{200}) \times (\Delta_v/\sigma_v)$ (see Noble et al. 2013). We consider galaxies that are probably infalling, or being recently accreted, galaxies in an intermediate bin, and a central bin with virialized objects (accreted earlier in the cluster formation). These regions are shown in dark orange, magenta, cyan and black in Fig. 14,

for the intervals $(R/R_{200}) \times (\Delta_v/\sigma_v) > 1.5$, $0.8 < (R/R_{200}) \times (\Delta_v/\sigma_v) \leq 1.5$, $0.2 < (R/R_{200}) \times (\Delta_v/\sigma_v) \leq 0.8$, and $(R/R_{200}) \times (\Delta_v/\sigma_v) \leq 0.2$, respectively. Note these regions are not precisely defined and serve for guidance only.

From Fig. 14 we can see a clear decrease in sSFR as we go from high to low values of the phase-space param-

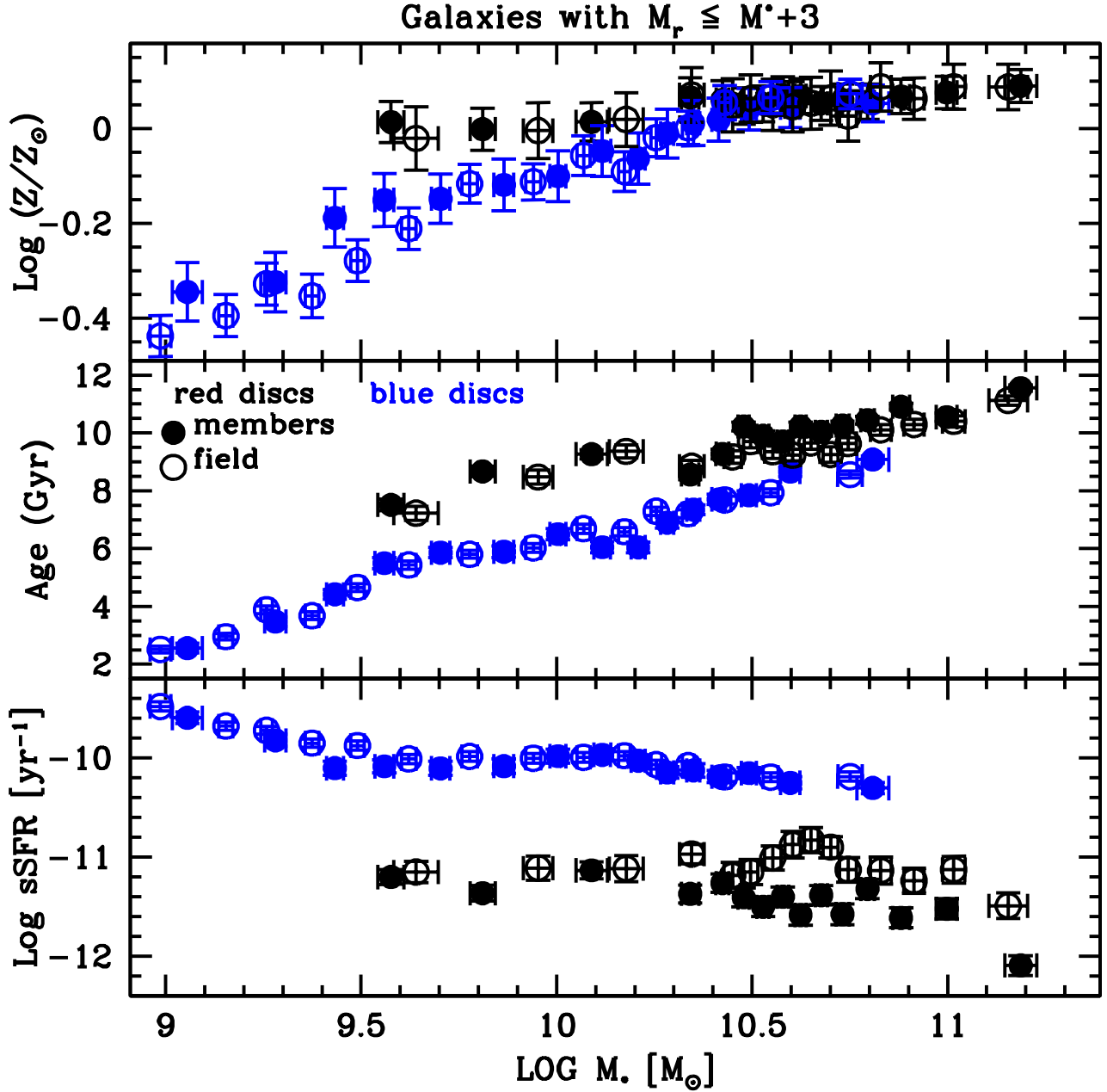


Figure 13. The relations between stellar metallicity (Z , top panel), the age of the stellar population (middle), and the sSFR (bottom) *vs* stellar mass, for the “blue discs” (blue points) and “red discs” (black points). Field galaxies are shown as open symbols and cluster objects as filled symbols. The error bars indicate the 1σ standard error on the biweight location estimate. We detect a clear metallicity difference between “red discs” and “blue discs”, from which we estimate a quenching time scale of $\sim 2\text{--}3$ Gyr.

ter $(R/R_{200}) \times (\Delta_v/\sigma_v)$, indicating that “red disc” galaxies halt the star formation when moving into the clusters. However, the strong dependence to stellar mass is still seen. For instance, for the most central bin (black points) the sSFR decreases from $\text{Log sSFR} \sim -11.2$ to $\text{Log sSFR} \sim -12.2$, at $9.7 < \text{Log } M_* < 11.2$.

Fig. 15 is analogous to Fig. 14, but now we also show field results, and divide the “red discs” in local galaxy density intervals, two for the field and three for cluster galax-

ies. The density ranges adopted are indicated in the figure. Open symbols are used for field results and filled symbols for cluster galaxies. This plot reinforces the conclusion from the previous figure, indicating that cluster “red discs” decrease their sSFR when reaching higher local density values (or smaller values of $(R/R_{200}) \times (\Delta_v/\sigma_v)$). However, now comparing to the field “red discs” we can see this population (open points) assumes a nearly constant value (and higher than for clusters), except for the most massive bin. Hence,

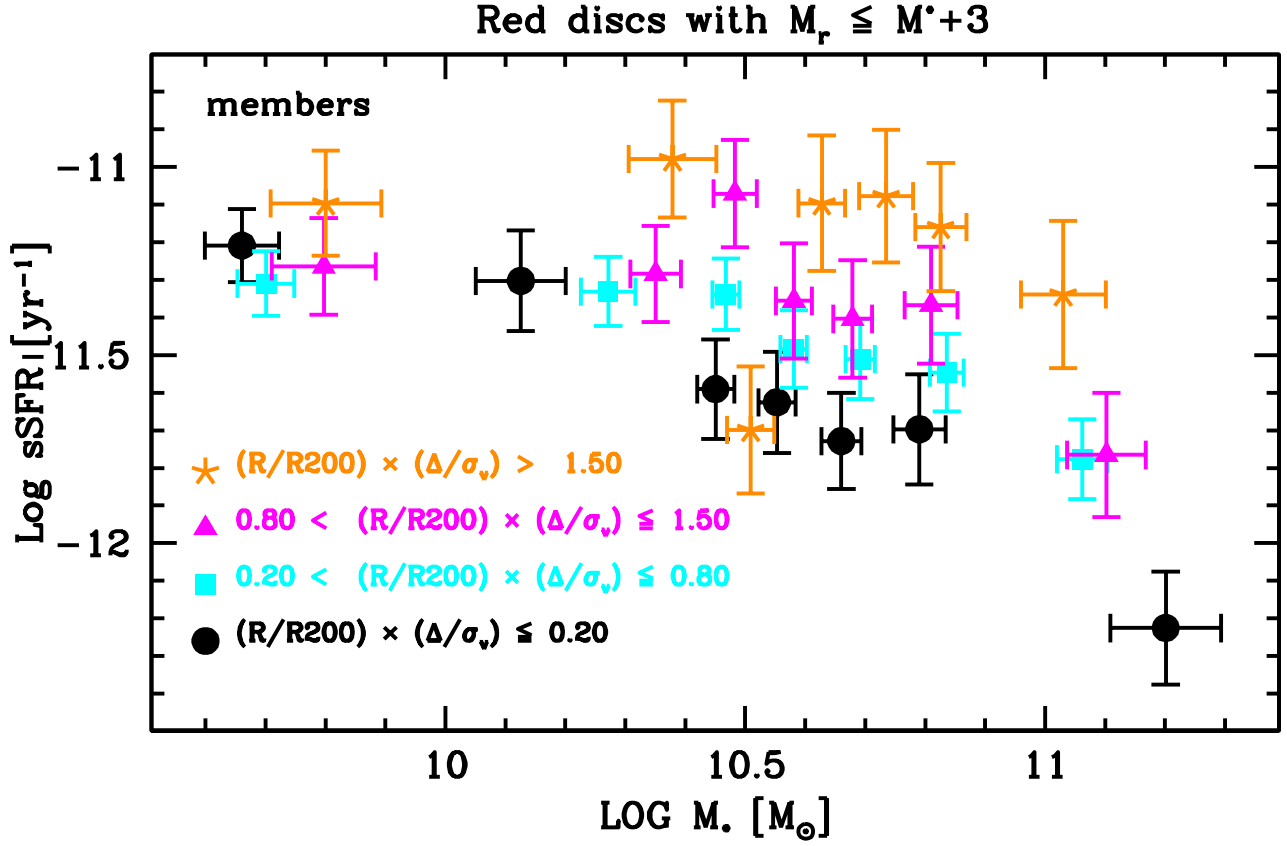


Figure 14. The sSFR– M_* relation for “red discs”, dividing the results in four ranges of the phase-space parameter $(R/R200) \times (\Delta_v/\sigma_v)$. We show in dark orange, magenta, cyan and black the results for the intervals $(R/R200) \times (\Delta_v/\sigma_v) > 1.5$, $0.8 < (R/R200) \times (\Delta_v/\sigma_v) \leq 1.5$, $0.2 < (R/R200) \times (\Delta_v/\sigma_v) \leq 0.8$, and $(R/R200) \times (\Delta_v/\sigma_v) \leq 0.2$, respectively. The error bars indicate the 1σ standard error on the biweight location estimate. “Red discs” decrease their sSFR as they move into clusters and grow in mass.

field “red discs” are not affected by local environment (except the most massive, $\text{Log } M_* > 10.8$). For cluster members the sSFR is sensitive to local density and stellar mass for objects more massive than $\text{Log } M_* = 10.4$. The variation with stellar mass is also more pronounced for objects in environments with $\text{Log } \Sigma_5 > 0.3$ (cyan and black points), which is roughly equivalent to $(R/R200) \times (\Delta_v/\sigma_v) \leq 0.8$ (from Fig. 14).

Fig. 16 is similar to Fig. 15, but we do not split the data

in density bins. We only compare field (open symbols) and cluster galaxies (filled symbols), but now besides showing the “red discs” (black points) we also exhibit the other three populations; “blue discs”, “blue bulges” and “red bulges”, in blue, green and red, respectively. Comparing to the “blue discs” and “red bulges” we reinforce the suggestion that “red discs” represent a transition population between the other two. As “blue discs” grow in mass they decrease their specific star formation rate. As they move into clusters, where other

mechanisms are common (such as *ram-pressure stripping*), this effect is probably enhanced. Hence, we could suggest the transformation of “blue discs” into “red discs” to be the combination of the stellar mass growth and environmental influence. Another interesting feature on this figure is the fact that only the red galaxies display differences between field and cluster results, especially the “red discs”.

5.2 The Star Formation Histories (SFH)

Another way to compare the two transitional galaxy populations (“red discs” and “blue bulges”) to the other galaxies (“blue discs” and “red bulges”) is through the use of their star formation history estimates. The STARLIGHT code derives the amount of star formation for a galaxy in several age bins. The current stellar mass of each galaxy is the result of adding the stellar mass formed on each age bin. We express the star formation history (SFH) of each galaxy as the fraction of stars formed on each age bin. Here we consider four wide age bins (as done by [Tojeiro et al. 2013](#)). Note the star formation fractions add up to unity over all cosmic history.

Fig. 17 shows the average star formation fractions (SFFs) as a function of lookback time for the four galaxy populations (“red discs”, “blue bulges”, “blue discs” and “red bulges”). Bulges are shown as filled symbols, and discs as open symbols. Blue galaxies are in blue and red objects in red. We also split cluster and field results, with the former in the top panel and the latter in the bottom. The four age intervals correspond to 0–0.05 Gyr, 0.05–0.5 Gyr, 0.5–2.5 Gyr, and > 2.5 Gyr.

From Fig. 17 we can see the recent star formation of “red discs” is smaller than the “blue discs” (by 10 to 12 times, if in the field or clusters), but is larger than the “red bulges”. The “red disc” population forms ~ 4 times more stars than “red bulges” in the recent Universe (< 100 Myr). Differences in the SFHs of red and blue discs are seen in all age bins, especially the most three recent. That indicates their SFHs are significantly different for at least ~ 2.5 Gyr. This result corroborates the quenching time scale we had estimated for the “blue discs” from Figs. 13–16. We also find field and cluster results to be very similar, except for the fact the field SFFs are slightly higher, especially for the two youngest bins. Finally, blue galaxies (bulges and discs) have very similar SFHs, except for the field, where “blue discs” form less stars in the two youngest bins. Note that our results are not directly comparable to the ones from [Tojeiro et al. \(2013\)](#) as they allow for more galaxy populations, dividing the spirals in blue and late types. They also restrict their analysis to massive galaxies ($\text{Log } M_* > 10.7$). However, we verified that there is no difference in our conclusions if we restrict the analysis to massive galaxies.

5.3 The Nature of Blue Bulges

The location of “blue discs” is very similar to the “blue bulges” in Fig. 16. The two populations show a decrease in the sSFR with stellar mass. Note the decrease would be even larger if we were showing the less massive objects ($\text{Log } M_* \leq 9.5$), as can be seen for “blue discs” in the bottom panel of Fig. 13. The two populations also show little difference between field and cluster results. The SFHs displayed in

Fig. 17 are also very similar for the two populations. Hence, despite the fact “blue discs” and “blue bulges” have different morphologies they do show similar SFR properties, but slight different distributions of age and metallicity. We then decided to investigate if part of the ongoing star formation in the “blue bulges” could be the result of mergers.

We do so as the visual inspection of the “blue bulges” indicates some of them show signs of interaction. We investigated this further estimating the asymmetry of these galaxies, and also comparing them to the “red bulges”. To derive asymmetry for these galaxies we used the public software PyCA ([Menanteau et al. 2013](#)). PyCA is a Python software designed to compute asymmetry (A) and concentration (C) from SExtractor products. Note the definition of concentration in PyCA is different from the SDSS, which we adopt for this work. More details on this software can be found in [Menanteau et al. \(2013\)](#). We computed the “A” parameter for all “blue bulges” and for comparison for a subset of “red bulges” (900 galaxies). The software is applied to the *r*-band images, which are deep enough and not too affected by local star formation.

We compared the asymmetry cumulative distributions of all “blue bulges” and the subset of “red bulges”, finding the former to be shifted to higher A values than the latter. As the two populations span different stellar mass ranges we then performed the comparison only for galaxies in a common mass range ($10.2 \leq \text{Log } M_* \leq 10.8$), as displayed in Fig. 18, in the top for cluster and in the bottom panel for field galaxies. Even for this small stellar mass range the differences between the asymmetry distributions for the two populations are easily seen. The comparison between cluster and field results in Fig. 18 also reveals no difference for the “red bulges”, but slightly higher asymmetry values for the “blue bulge” cluster population. That reinforces the discussion related to Fig. 9 (§ 4), where we argue that “blue bulges” in the field and in clusters may be composed of different subtypes of galaxies. That could be one reason explaining higher *Z* values for “blue bulges” in clusters.

From the visual inspection of extreme cases (low and high asymmetry) of red and blue bulges we find the following. In many cases the “blue bulges” show clear signs of strong interaction, indicating wet mergers. However, in some cases they look like very asymmetric low mass spiral galaxies dominated by a bulge. On the other hand, for the “red bulges” with high A values, when the asymmetry is clearly distinguishable they only display signs of dry mergers.

For the galaxies with low asymmetry, both populations (“blue bulges” and “red bulges”) look like “spheroidal” or bulge dominated systems. In particular, the “blue bulges” are small and often display a starburst spectrum. Hence, we can say that from low to high asymmetry the “blue bulges” can be simple spheroids, or bulge dominated low mass spirals, or wet mergers. However, it is important to stress that this visual inspection we perform is not the main goal of the current work (as we discussed in § 2.6). In particular, the “blue bulges” are generally faint low mass systems, making their visual classification harder. When we say some of them look like very asymmetric spiral galaxies, that does not mean we are referring to large massive early spirals.

Considering the asymmetry value we also compared the specific star formation rate *vs* stellar mass plane of low and high A “blue bulges”. That is displayed in Fig. 19. We can see

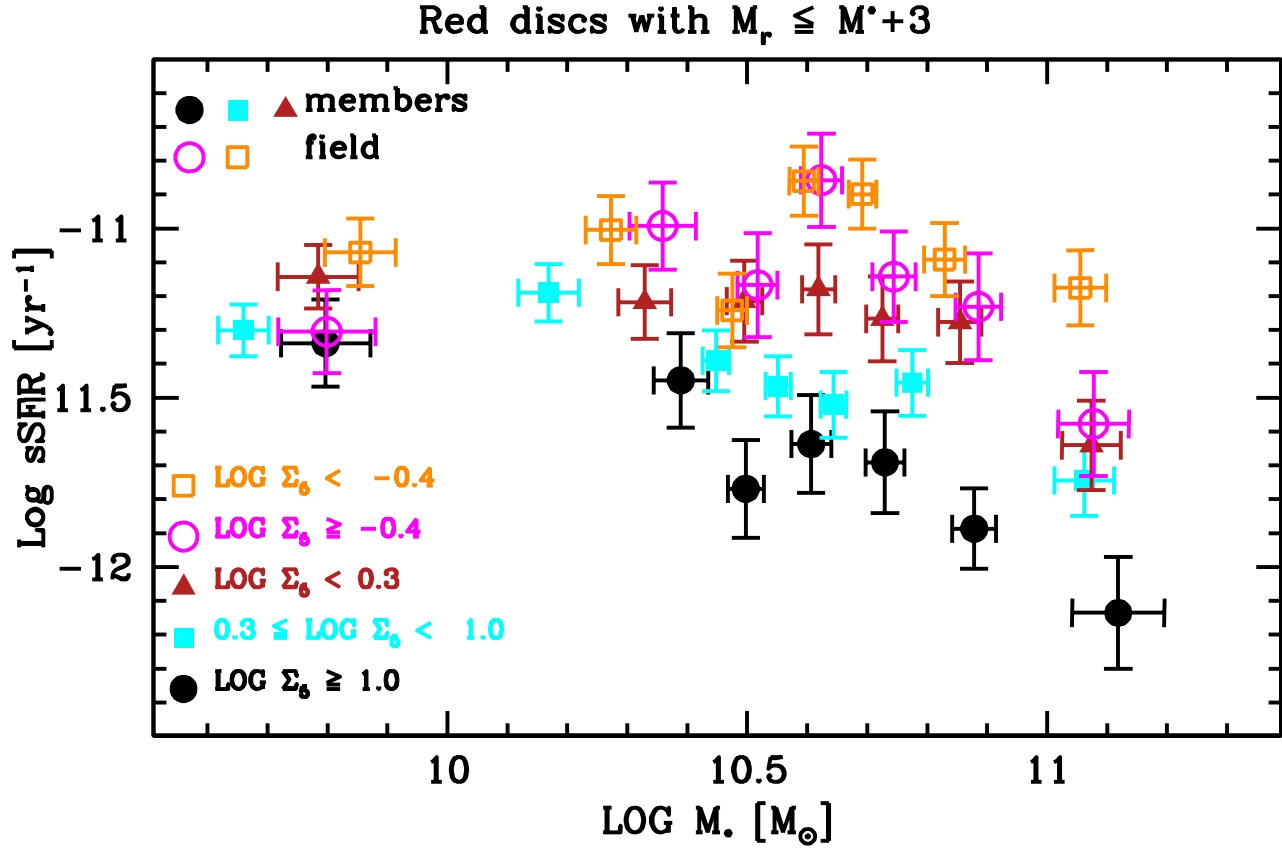


Figure 15. Analogous to Fig. 14, but now also showing field results, and dividing the “red discs” in local galaxy density intervals, two for the field and three for cluster galaxies. In the field “red discs” are shown by open symbols, in dark orange and magenta for the intervals $\text{Log } \Sigma_5 < -0.4$ and $\text{Log } \Sigma_5 \geq -0.4$, respectively. Member galaxies are displayed by filled symbols, in brown, cyan and black, for the intervals $\text{Log } \Sigma_5 < 0.3$, $0.3 \leq \text{Log } \Sigma_5 < 1.0$ and $\text{Log } \Sigma_5 \geq 1.0$, respectively. The error bars indicate the 1σ standard error on the biweight location estimate. Except for the most massive, field “red discs” are not affected by local environment. On the contrary, for cluster members the sSFR is sensitive to local density and stellar mass for objects more massive than $\text{Log } M_* = 10.4$.

a significant difference in the sSFR of low and high A “blue bulges” at $9.5 < \text{Log } M_* < 10.5$ (note that does not happen at all masses), with high A galaxies displaying higher sSFR values. That indicates these mergers contribute to make part of the the “blue bulge” population more active than the rest. A similar comparison, but using H δ (instead of sSFR), also reveals differences between low and high A “blue bulges”, in-

dicating the presence of young stellar populations (< 1 Gyr) among the most asymmetrical “blue bulges”. A similar plot using metallicity ($Z-M_*$) shows no significant difference, reinforcing the SFR enhancement is recent.

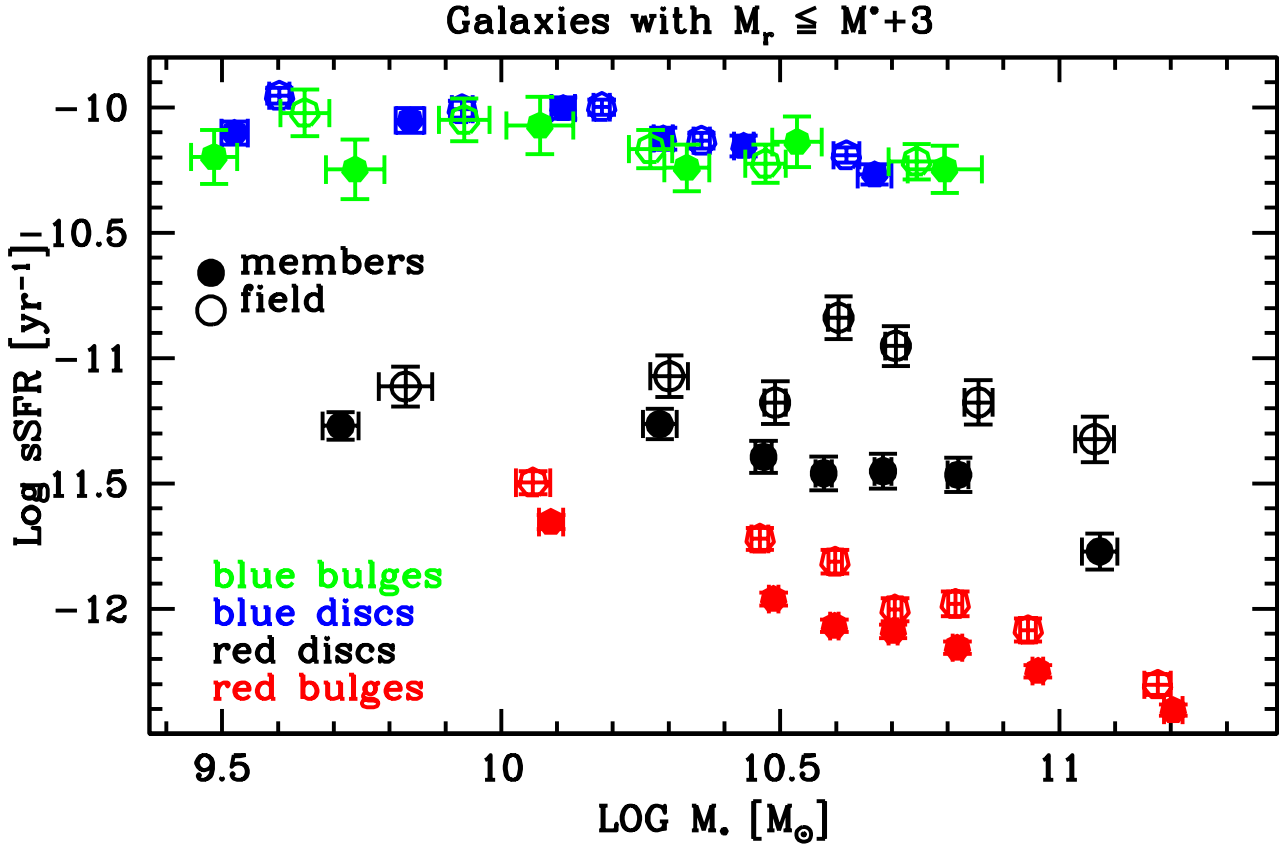


Figure 16. Analogous to Fig. 15, but now also showing the other three populations (“blue discs”, “blue bulges” and “red bulges”), and not splitting the data in density bins. For each galaxy population field results are shown by open symbols, while members are displayed by filled symbols. The error bars indicate the 1σ standard error on the biweight location estimate. In the stellar mass range of this figure only the red galaxies decrease the sSFR as they grow in mass. Those objects are also the only ones to display differences between field and cluster results, especially the “red discs”.

6 DISCUSSION

Several different works in the literature aim to investigate transitional galaxies and to assess the time scale for quenching star formation (Wolf et al. 2009; Muzzin et al. 2014; Vulcani et al. 2015; Haines et al. 2013, 2015; Tojeiro et al. 2013; Roberts et al. 2016). Many results point to a slow quenching scenario on which processes like strangulation

are predominant (Peng et al. 2015; Roberts et al. 2016; Maier et al. 2016). On top of that the importance of the cluster environment has been strengthened, especially by studies based on the investigation of galaxy properties in the phase-space (Noble et al. 2013, 2016; Haines et al. 2013, 2015; Maier et al. 2016).

Haines et al. (2013) find the specific SFRs of massive central star-forming galaxies (within R200) to be much lower

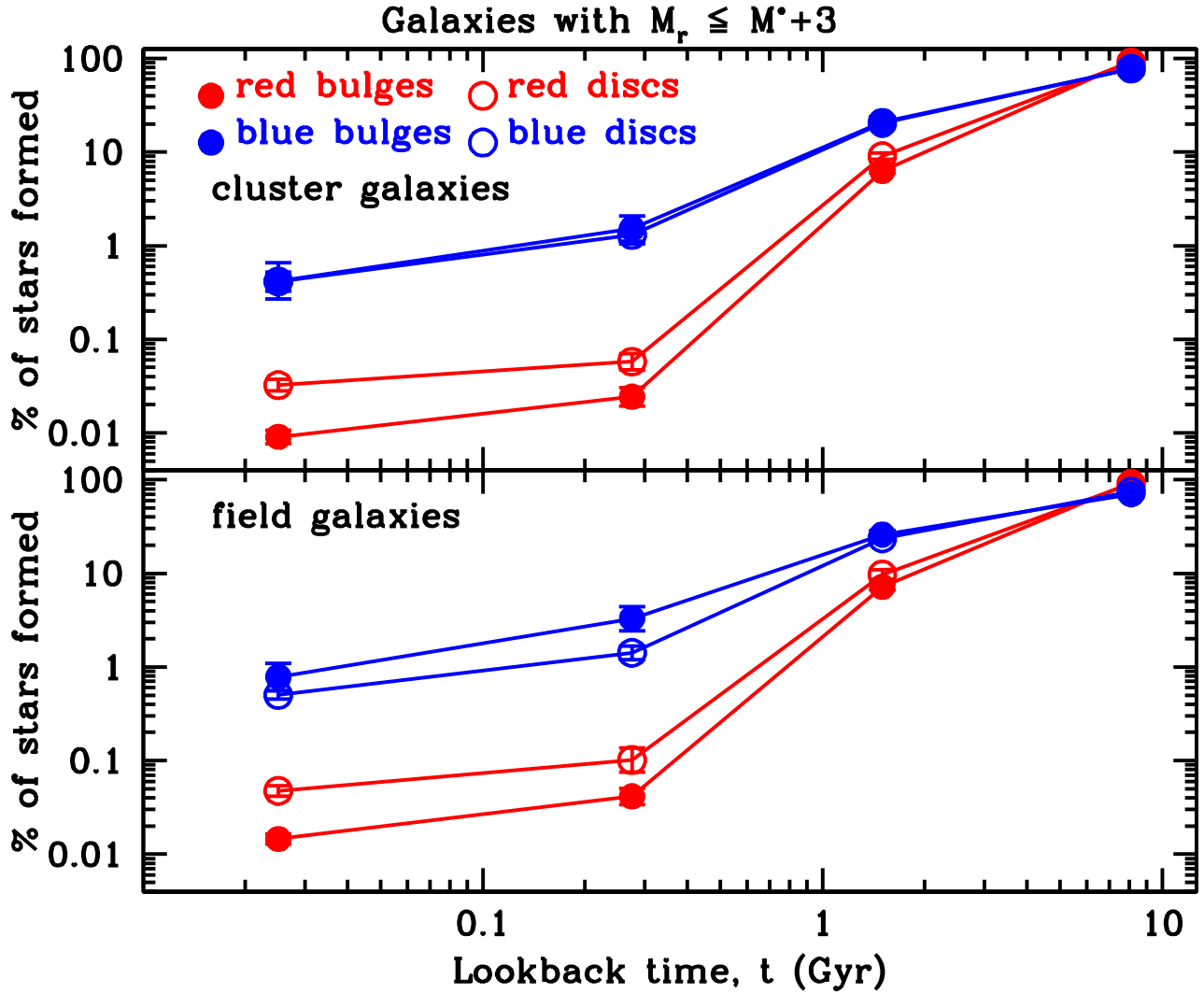


Figure 17. The star formation history (average star formation fraction as a function of lookback time) for the four galaxy populations in the current work. Red galaxies are displayed in red, and blue galaxies in blue. Bulges are shown as filled symbols, while discs are exhibited as open symbols. The top panel shows the results for cluster galaxies, while the field is in the bottom. The four age intervals correspond to 0–0.05 Gyr, 0.05–0.5 Gyr, 0.5–2.5 Gyr, and > 2.5 Gyr. The error bars indicate the 1σ standard error on the biweight location estimate. The “red discs” form ~ 4 times more stars than “red bulges” in the recent Universe (< 100 Myr). The SFHs of red and blue discs are significantly different for at least ~ 2.5 Gyr, corroborating the quenching time scale estimated after Figs. 13–16.

than the field counterpart. They take that as an indication of slow quenching (timescales of 0.7–2.0 Gyr) of massive SF galaxies once arriving in clusters. Haines et al. (2015) verify the surface density of SF to have a steep decline with radius, implying that recently accreted spirals will maintain star formation for 2–3 Gyr. They also compare the phase-space diagram of SF galaxies with results from the Millennium

simulation, concluding the quenching time scale to be ~ 1.7 Gyr.

Although we are mainly interested in transitional galaxies (in particular “red discs” as an intermediate population between the blue cloud and red sequence), our conclusions are in good agreement to those above. From Figs. 13–17 we have different indications that the star formation quenching

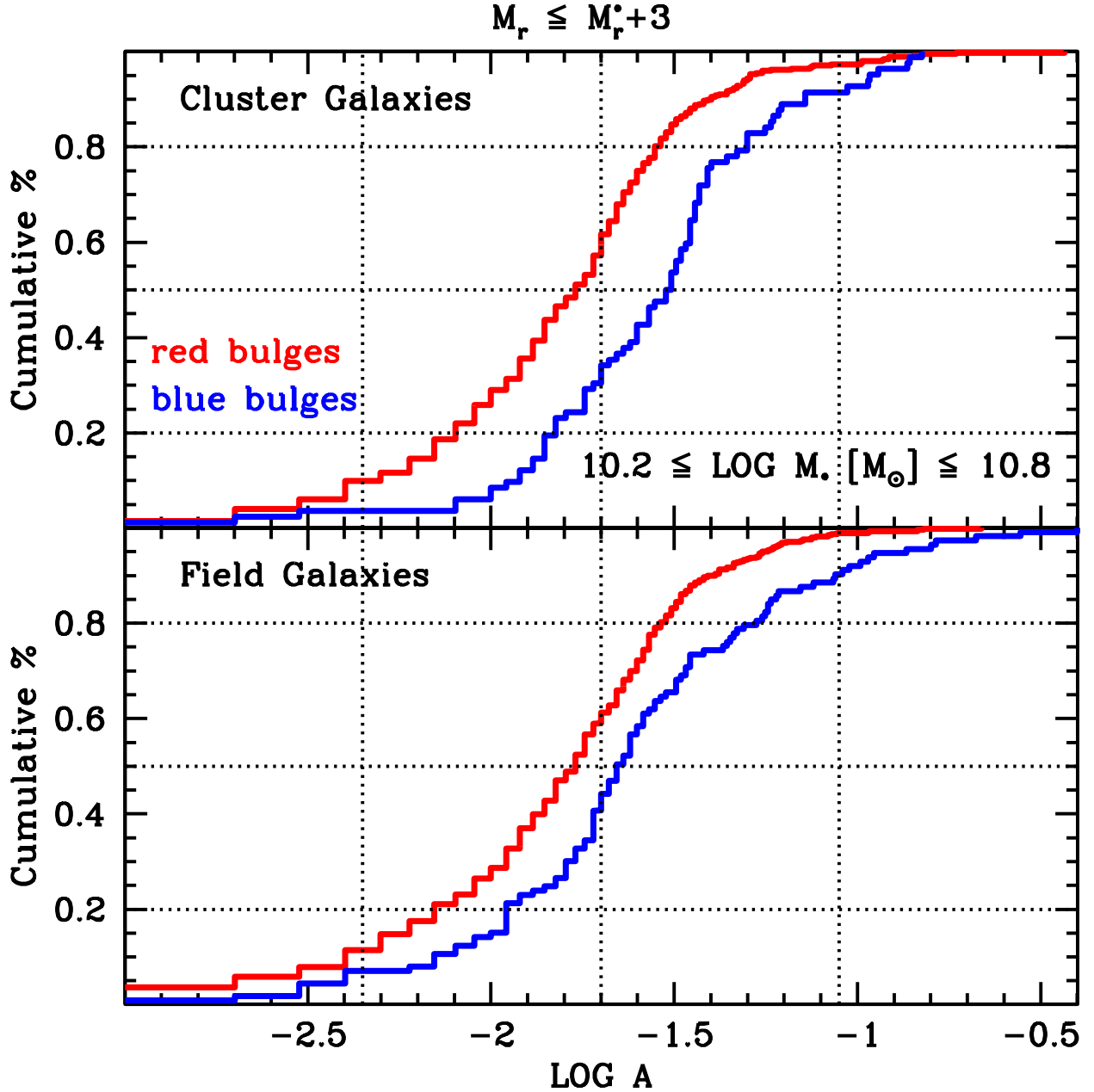


Figure 18. The cumulative distribution of the asymmetry (A) parameter for the red and blue bulges at $10.2 \leq \text{Log } M_* \leq 10.8$. In the top the comparison considers cluster galaxies, while in the bottom only field galaxies. Even for this small stellar mass range we clearly see the “blue bulge” population show larger values of the asymmetry (A) parameter.

is slow (~ 2 Gyr) and depends on stellar mass, but also on environment. The metallicity difference as a function of stellar mass, between “red discs” and “blue discs”, is consistent to a quenching time scale of 2–3 Gyr for field and cluster galaxies.

From Fig. 17 we conclude “red discs” have residual star formation compared to the “blue discs”, but still forms ~ 4 times more stars than “red bulges” in recent times (< 100 Myr). The comparison of the SFHs of “red discs” and “blue discs” lead us to the conclusion their SFH are significantly

different for at least ~ 2.5 Gyr. All these facts, plus the distributions of SFR, $12\mu\text{m}$ luminosity, L_{dust} and sSFR, indicate the red and blue discs are distinct populations, with the former possibly representing the transition to “red bulges”. This transition is slow, with quenching time scales of > 2 Gyr. Morphological transformations would happen even in a longer time scale, which is also in good agreement to a scenario requiring pre-processing in groups (Haines et al. 2015; Lopes, Ribeiro & Rembold 2014). In the pre-processing scenario galaxy transformations could be divided in two steps

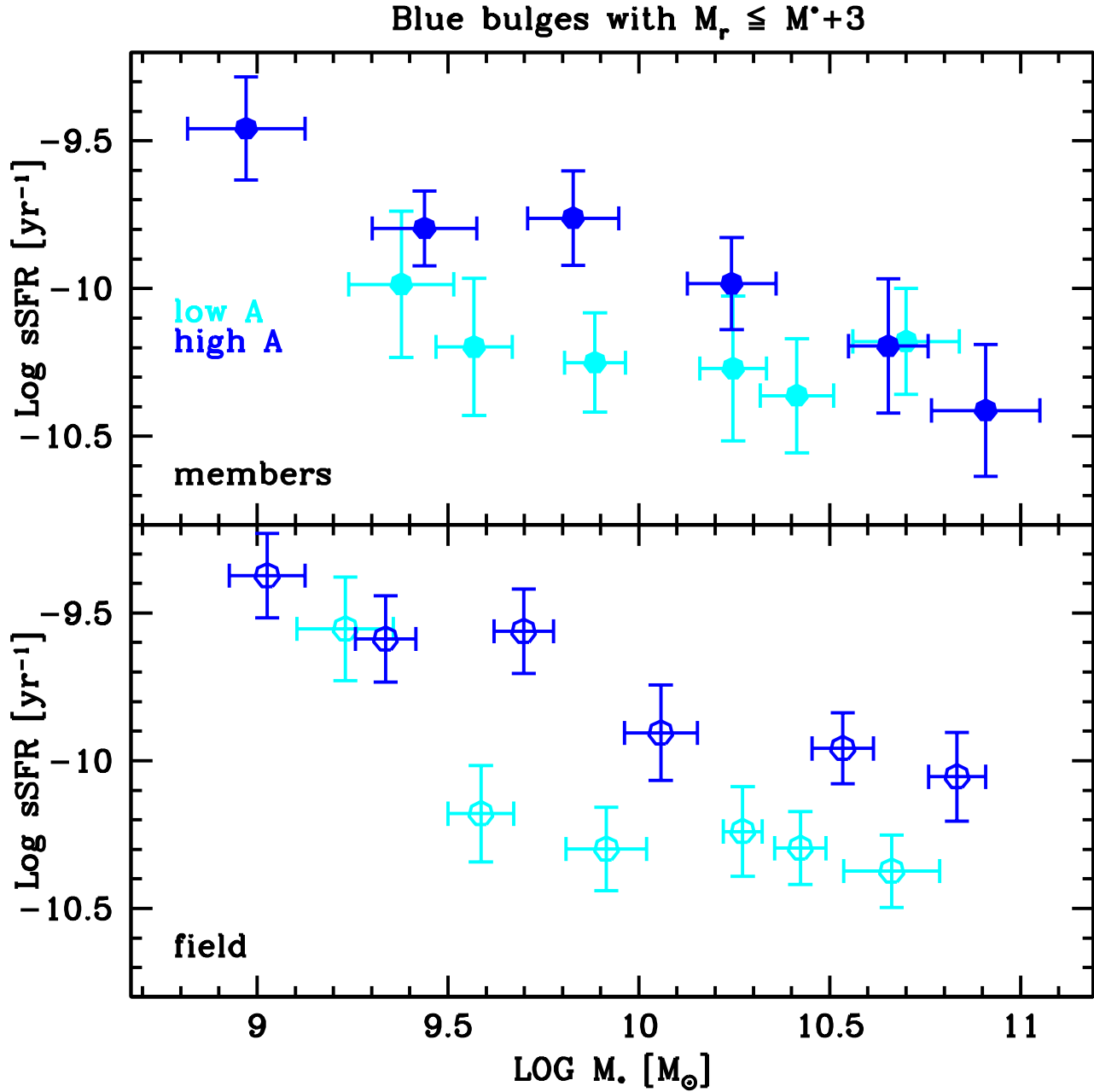


Figure 19. The sSFR *vs* M_* plane for “blue bulges” classified as low (cyan points) and high (blue points) asymmetry. In the top the comparison considers cluster galaxies, while in the bottom only field galaxies. At $9.5 < \text{Log } M_* < 10.5$ there is a significant difference in the sSFR of low and high A “blue bulges”, with highly asymmetrical galaxies having higher sSFR values.

(Lackner & Gunn 2013), where star formation is quenched in the group scale, but morphological transformation is a separate process, occurring in clusters. First, star formation is halted in discs residing in relatively low-density environments. Secondly, a morphological transformation from disc to bulge-dominated systems occur at higher densities.

Figs. 14–16 clearly point to the importance of the cluster environment to decrease the sSFR of the transitional galaxies called “red discs”. In Figs. 15–16 we can also detect the difference between field and cluster results for the “red

disc” population. The global picture is that “blue discs” decrease their specific star formation rate as they grow in mass and as they infall into galaxy clusters. We can see (Fig. 15) a clear difference between field (dark orange and magenta points) and cluster (brown, cyan and black points) results for the “red discs”. On top of that we detect a significant dependence with local density for the massive cluster “red discs” ($\text{Log } M_* > 10.5$).

On Fig. 16 we can also see the variation of the sSFR with stellar mass for the “red bulges” (varying from Log

sSFR ~ -11.5 to $\text{Log sSFR} \sim -12.5$, at $10.0 < \text{Log } M_* < 11.5$). It is also possible to notice the difference between field (open symbols) and cluster results (filled points) for the “red bulges”. That is not true for the star-forming blue galaxies (“blue discs” and “blue bulges”). We can not detect a significant difference between field and cluster results, and only a small variation of sSFR with stellar mass. A large variation exists only for lower mass galaxies ($\text{Log } M_* < 9.5$), as can be seen in the bottom panel of Fig. 13. These results are in good agreement to what is seen in Haines et al. (2013). They find a significant difference in the sSFR vs M_* relation for field and cluster massive star-forming galaxies, but only when using members within R_{200} . If the cluster sample is from the infall region, field and cluster results agree. We do not make an environmental distinction within clusters for the blue galaxies (discs and bulges); so that the good agreement we see to the field is probably due to predominance of these SF blue galaxies in the lower density infall regions of clusters (closer in density to the field values).

This similarity between “blue discs” and “blue bulges” seen on the sSFR– M_* relation (Fig. 16) is also detected in several other properties (see, for instance, Figs. 2, 8, 15, 17). Although these two populations seem to have similar SFR and dust luminosity, they display slightly different distributions of age, metallicity and stellar mass for bright galaxies (Fig. 9). They also display different dependence on environment for the sSFR distributions seen in Fig. 11. However, it is important to stress that blue bulges and discs similarities are much more pronounced than their differences. Except for morphology “blue bulges” are much closer to “blue discs” than to “red bulges”. Vulcani et al. (2015) suggest that blue star-forming early-types (BSF) could be the result of a morphological transformation happening before the star formation is halted, with the stellar disc being removed entirely or at least in part. On the other hand, Tojeiro et al. (2013) argue that the differences in the dust content between blue ellipticals and spirals is an indication the former are not descendants of the blue spirals. Another possibility is that these blue early-type galaxies be the result of rejuvenation, through the merger with a star forming galaxy. Salim & Rich (2010) suggest this rejuvenation scenario is plausible from the analysis of optically quiescent early-type galaxies with strong UV excess. Kannappan et al. (2009) argue that blue E/S0 individual galaxies may be evolving either up to red sequence or down into the blue cloud. They also argue those galaxies represent a transitional class. The most massive resemble major-merger remnants that will end up in the red sequence, while lower mass objects ($M < 3 \times 10^{10} M_\odot$) display signs of disk and/or pseudobulge building. The case for lower mass galaxies is reinforced by the results of Wei et al. (2010), who investigated low mass blue-sequence E/S0 galaxies. They argue these low mass galaxies are more common in low-density field environments where fresh gas infall is possible. They find evidence that star formation is bursty, involving externally triggered gas inflows. They also suggest most of these galaxies can grow stellar disks on relatively short timescales.

As stated above we do find evidence for mergers within the “blue bulges” sample, both from their visual inspection and the analysis of asymmetry (see Figs. 18 and 19). However, in some cases the high asymmetry “blue bulges” simply resemble asymmetric low mass spiral galaxies dominated by

a bulge. An interesting point is that we find evidence that high A “blue bulges” have an enhanced star formation compared to the more regular galaxies (see Fig. 19). To summarize, from low to high asymmetry we find “blue bulges” that are spheroids, bulge dominated low mass spirals, or resemble wet mergers. Hence, quoting Tojeiro et al. (2013), there may not be a single evolutionary path for the blue early-type objects. As Kannappan et al. (2009) suggest some of these objects may be going up to the red sequence, while others are going in the opposite direction towards the blue cloud.

7 SUMMARY

In this work we measure the typical environment of transitional galaxy populations selected solely by photometric parameters (color and concentration). Those galaxies are called “red discs” and “blue bulges”. We compare the environments of these galaxies to normal objects from the blue cloud and red sequence, which we select as “red bulges” and “blue discs”. Besides comparing environmental related parameters (such as crossing time and Σ_5), we also compare physical properties like age and metallicity. We also used the cumulative distributions of different properties of these galaxy populations to assess the impact of stellar mass and environment (local and global). Then we investigate the location of these populations in the $Z-M_*$, Age– M_* and sSFR– M_* planes, and analyze their SFHs. Doing so, we suppose possible galaxy evolutionary scenarios and estimate the quenching time for “blue discs”. Finally, we estimate the asymmetry of the “blue bulges”, trying to assess the impact of mergers on this population. Our main results are:

- (i) At fixed morphology we see the number of “red discs” (“blue bulges”) relative to the number of discs (bulges) vary strongly with local density, especially in the cluster environments (Figs. 3, 4, 5, 6). The transformation happens mainly within the virial radius.
- (ii) As a function of distance to the cluster center we find the two populations to be nearly constant from the outskirts to R_{200} . Inwards, the relative numbers decrease (increase) for the “blue bulges” (“red discs”), for bright and faint galaxies. Such results give strength to the importance of clusters to transform galaxy properties (Figs. 5, 6).
- (iii) Dividing the sample in stellar mass bins we see this environmental variation is most significant for the lower mass bins ($\text{Log } M_* \leq 10.6$), reinforcing that star formation is halted first in higher mass objects (Fig. 7).
- (iv) Galaxies of the same color, but different morphologies (discs or bulges) show little difference in their typical environment. However, that is not true if morphology is fixed, instead of color. Red and blue discs are found in very different environments, stressing these two populations are indeed different. Red objects have shorter crossing times and are at higher densities than blue galaxies (Fig. 8).
- (v) Although found at similar environments “red bulges” have an older stellar population and higher metallicities than “red discs” (Fig. 9).
- (vi) The SFR of red and blue discs is very different, and the former shows higher values than the passive “red bulges” (Fig. 2).
- (vii) On what regards dust luminosity “blue bulges” have slightly lower values than “blue discs”, which have much

larger L_{dust} than “red discs”. Nonetheless, the later still shows higher L_{dust} values than “red bulges” (Fig. 10).

(viii) From the cumulative distributions of sSFR we see no overlap of blue and red populations, and “red discs” and “red bulges” are different in all environments. We also find the largest variations with local density for the red objects at fixed morphology (mainly for the “red discs” within clusters). Finally, local galaxy density seems to affect more those distributions than the global environment (Fig. 11).

(ix) A similar analysis in different stellar mass ranges reveals this parameter to be even more important to galaxy properties when compared to Σ_5 . The largest variations are again seen for “red discs”, suggesting those galaxies halt star-formation as increasing their mass and moving into clusters. Hence, both local and global environment matter (local being more important). But the most effective parameter to shape all four galaxy populations is stellar mass (Fig. 12).

(x) The metallicity difference, as function of stellar mass, between “red discs” and “blue discs” is consistent to a slow quenching scenario, with a time scale of 2–3 Gyr for field and cluster galaxies. This time scale is corroborated by the analysis of the star formation histories of the different galaxy populations. The SFHs of “red discs” and “blue discs” should differ for at least ~ 2.5 Gyr (Figs. 13, 17).

(xi) The distribution of “red discs” in the sSFR– M_* plane for different environments reveals this population to gradually change as they move into clusters. That is seen in Figs. 14, 15 and 16. The first figure shows the results in phase-space bins, the second in local density bins (also comparing field and cluster “red discs”). The third figure compares field and cluster galaxies, but also displaying the other three populations.

(xii) Fig. 16 is also important to reinforce the idea that “red discs” are the descendants of “blue discs”, on their way to become a passive population.

(xiii) We found that part of the “blue bulges” can be explained by wet mergers, as indicated by their visual inspection and asymmetry values (Fig. 18). In particular, the high asymmetry “blue bulges” have larger sSFR and $H\delta$ values, indicating the presence of young stellar populations (Fig. 19).

(xiv) We do not conclude on a single evolutionary path for the “blue bulge” population, as we find they may be simple spheroids, low mass bulge dominated spirals, or resemble wet mergers.

ACKNOWLEDGEMENTS

ALBR thanks for the support of CNPq, grants 306870/2010-0 and 478753/2010-1. PAAL thanks the support of CNPq, grant 308969/2014-6.

This research has made use of the SAO/NASA Astrophysics Data System, and the NASA/IPAC Extragalactic Database (NED). Funding for the SDSS and SDSS-II was provided by the Alfred P. Sloan Foundation, the Participating Institutions, the National Science Foundation, the U.S. Department of Energy, the National Aeronautics and Space Administration, the Japanese Monbukagakusho, the Max Planck Society, and the Higher Education Funding Council for England. A list of participating institutions can be obtained from the SDSS Web Site <http://www.sdss.org/>.

REFERENCES

- Berlind A., Frieman J., Weinberg D. et al. 2006, *ApJS*, 167, 1
 Brinchmann J. et al. 2004, *MNRAS*, 351, 1151
 Bundy K. et al. 2006, *ApJ*, 651, 120
 Caputi K.I. et al. 2006, *A&A*, 454, 143
 Caputi K.I. et al. 2009, *ApJ*, 707, 1387
 Chang Y., van der Wel A., da Cunha E., Rix H. 2015, *ApJS*, 219, 8
 Cid Fernandes R., Mateus A., Sodrál L., Stasinska G., & Gomes J.M. 2005, *MNRAS* 358, 363
 Cimatti A., Daddi E., Renzini A. 2006, *A&A*, 453, 29
 Cowie L.L. et al. 1996, *AJ*, 112, 839
 Crawford S.M., Wirth, G.D., Bershad, M.A. 2014, *ApJ*, 786, 30
 Crossett J.P. et al. 2014, *MNRAS*, 437, 2521
 da Cunha E., Charlot S. & Elbaz D. 2008, *MNRAS*, 388, 1595
 da Cunha E. et al. 2013, *ApJ*, 765, 9
 Djorgovski S.G., de Carvalho R.R., Gal R.R., Odewahn S.C., Mahabal A.A., Brunner R.J., Lopes P.A.A., Kohl Moreira J.L. 2003, *Bulletin of the Astronomical Society of Brazil*, 23, 197
 Dressler A. 1980, *ApJ*, 236, 351
 Dressler A., Gunn J.E. 1983, *ApJ*, 270, 7
 Dressler A., & Shectman S.A. 1988, *AJ*, 95, 985 (DS)
 Fadda D., Girardi M., Giuricin G., et al. 1996, *ApJ*, 473, 670
 Fontanot F. et al. 2009, *MNRAS*, 397, 1776
 Gal R.R., de Carvalho R.R., Lopes P.A.A., Djorgovski S.G., Brunner R.J., Mahabal A.A., Odewahn S.C. 2003, *AJ*, 125, 2064
 Gal R.R., de Carvalho R.R., Odewahn S.C., Djorgovski S.G., Mahabal A.A., Brunner R.J., Lopes P.A.A. 2004, *AJ*, 128, 3082
 Gal R.R., Lopes P.A.A., de Carvalho R.R., Kohl-Moreira J.L., Capelato H.V., Djorgovski S.G. 2009, *AJ*, 137, 2981
 Goto T. 2005, *MNRAS*, 357, 937
 Guglielmo V. et al. 2015, *MNRAS*, 450, 2749
 Haines C.P. et al. 2007, *MNRAS*, 381, 7
 Haines C.P. et al. 2013, *ApJ*, 775, 126
 Haines C.P. et al. 2015, *ApJ*, 806, 101
 Holden B.P. et al. 2012, *ApJ*, 749, 96
 Kannappan S.J. et al. 2009, *AJ*, 138, 579
 Kauffmann G., White S., Heckman T. et al. 2004, *MNRAS*, 353, 713
 La Barbera F., Lopes P.A.A., de Carvalho R.R., de La Rosa I.G., Berlind A.A. 2010, *MNRAS*, 408, 1361
 Lackner C.N., & Gunn J.E. 2013, *MNRAS*, 428, 2141
 Lintott C. et al. 2008, *MNRAS*, 389, 1179
 Lopes P.A.A., de Carvalho R.R., Gal R.R., Djorgovski S.G., Odewahn S.C., Mahabal A.A., Brunner R.J. 2004, *AJ*, 128, 1017
 Lopes P.A.A., de Carvalho R.R., Capelato H.V., Gal R.R., Djorgovski S.G., Brunner R.J., Odewahn S.C., Mahabal A.A. 2006, *ApJ*, 648, 209
 Lopes P.A.A. 2007, *MNRAS*, 380, 1680
 Lopes P.A.A., de Carvalho R.R., Kohl-Moreira J.L., Jones C. 2009a, *MNRAS*, 392, 135, paper I
 Lopes P.A.A., de Carvalho R.R., Kohl-Moreira J.L., Jones C. 2009b, *MNRAS*, 399, 2201, paper II
 Lopes P.A.A., Ribeiro A.L.B., Rembold S.B., 2014, *MNRAS*, 437, 2430, paper IV
 Maier C. et al. 2016, *arXiv:1602.00686*
 Masters K. et al. 2010, *MNRAS*, 404, 792
 McIntosh D.H. et al. 2014, *MNRAS*, 442, 533
 Menanteau F. et al. 2006, *AJ*, 131, 208
 Muldrew S., Croton D., Skibba R. et al. 2012, *MNRAS*, 419, 2670
 Muzzin A. et al. 2014, *ApJ*, 796, 65
 Noble A.G. et al. 2013, *ApJ*, 768, 118
 Noble A.G. et al. 2016, *ApJ*, 816, 48
 Odewahn S.C., de Carvalho R.R., Gal R.R., Djorgovski S.G., Brunner R.J., Mahabal A.A., Lopes P.A.A., Kohl Moreira J.L., Stalder B. 2004, *AJ*, 128, 3092
 Oemler A. 1974, *ApJ*, 194, 1

- Peng Y., Maiolino R., Cochrane R. et al. 2015, *Nature*, 521, 192
- Ribeiro A.L.B., Lopes P.A.A. & Rembold S.B. 2013, *A&A*, 556, 74, paper III
- Rines K. & Diaferio A. 2006, *ApJ*, 132, 1275
- Roberts I.D., Parker L.C., Karunakaran A. 2016, *MNRAS*, 455, 3628
- Salim S. et al. 2007, *ApJS*, 173, 267
- Salim S. et al. 2009, *ApJ*, 700, 161
- Salim S. & Rich R.M. 2010, *ApJ*, 714, 290
- Smethurst R.J. et al. 2015, *MNRAS*, 450, 435
- Soifer B.T. et al. 1984, *ApJ*, 278L, 71
- Strateva I., Ivezić Z., Knapp G. et al. 2001, *AJ*, 122, 1861
- Strauss M., Weinberg D., Lupton R. et al. 2002, *AJ*, 124, 1810
- Swinbank A.M. et al. 2012, *MNRAS*, 420, 672
- Tojeiro R. et al. 2013, *MNRAS*, 432, 359
- Tortora C. et al. 2010, *MNRAS*, 407, 144
- Tran K.H. et al. 2003, *ApJ*, 599, 865
- Valentinuzzi T. Poggianti B., Fasano G. et al. 2011, *A&A*, 536, 34
- Vulcani B. et al. 2015, *ApJ*, 798, 52
- Wei L.H. et al. 2010, *ApJ*, 725L, 62
- Wolf C. et al. 2009, *MNRAS*, 393, 1302
- Wuyts S. et al. 2007, *ApJ*, 655, 51
- Wyder T.K. et al. 2007, *ApJS*, 173, 293
- Yee H. & López-Cruz O., 1999, *AJ*, 117, 1985
- Zabludoff A.I. et al. 1996, *ApJ*, 466, 104

This paper has been typeset from a \LaTeX file prepared by the author.